Establishing Human Ileal Enteroids as an Alternative Model to Study *Vibrio cholerae* Pathogenesis

A thesis submitted by

Mary Hahm

in partial fulfillment of the requirements for the degree of

Master of Science

in

Molecular Microbiology

Tufts University

Sackler School of Graduate Biomedical Sciences

August 2019

Advisor: Wai-Leung Ng, PhD

Abstract.

Cholera is the secretory diarrheal disease caused by the bacterium *Vibrio cholerae*. Current laboratory models for studying *V. cholerae* infection include the infant mouse, the infant rabbit, and Caco-2 cell culture models. While these existing models are useful, they all have their limitations and prevent us from fully understanding the pathogenesis of *V. cholerae*. For example, infant mice do not experience watery diarrheal symptoms as humans do. Caco-2 cells are derived from colon adenocarcinoma, but *V. cholerae* is known to infect the small intestine. Thus, there is a need for an alternative model to study *V. cholerae* in a system that is more physiologically relevant to human infection. Enteroids are a promising cell culture technology to study host-pathogen interactions and have been successfully used to study several other gastrointestinal pathogens. Enteroids are derived from isolated crypts of the human small intestine and represent major differentiated cell types. Here, I use ileal enteroids seeded on 2D transwells to mimic the polarized epithelial monolayers of the small intestine as a novel system for studying early association and infection dynamics of *V. cholerae*. Wild-type *V. cholerae* associates and replicates on differentiated enteroid monolayers. Importantly, the association appears to be specific. A well-characterized mutant strain lacking the master quorum-sensing regulator LuxO, which is severely deficient for colonization in the infant mouse model, is also deficient for association and replication with the enteroid monolayers. Confocal immunofluorescence microscopy was used to quantify and localize the associated bacteria. Wild-type *V. cholerae* associates with monolayers as individual bacteria and small clusters resembling microcolonies, which have been observed inside animal hosts. Heterogeneity is observed in the infecting population. Previously reported cholera toxin-

induced damage to tight junctions was not observed post-infection with *V. cholerae* at early time points. In 3D enteroids, cholera toxin induces enteroid swelling, likely via chloride ion movement through the CFTR channel, and dramatically induces Mucin-2 levels. These results suggest that 2D and 3D enteroid systems can be used to help fill gaps in knowledge about early infection dynamics and human small intestinal epithelial cell damage induced by *V. cholerae*.

Table of Contents

List of Tables

List of Figures

List of Copyrighted Materials Used

T. Sato *et al.*, "Long-term Expansion of Epithelial Organoids from Human Colon, Adenoma, Adenocarcinoma, and Barrett's Epithelium," *Gastroenterology*, vol. 141, no. 5, pp. 1762–1772, Nov. 2011.

List of Abbreviations

ADP	Adenosine diphosphate
AMP	Adenosine monophosphate
BMP	Bone morphogenetic protein
BSA	Bovine serum albumin
C	Celsius
cDNA	Complementary deoxyribonucleic acid
CFTR	Cystic fibrosis transmembrane conductance regulator
CFU	Colony forming units
ChgA	Chromogranin A
$CMGF^{+}$	Conditioned medium with growth factors
$CMGF^{-}$	Conditioned medium without growth factors
CO_2	Carbon dioxide
CTX	Cholera toxin
DAPI	(4'6-diamidino-2-phenylindole)
ddH_2O	Double distilled water
DMEM	Dulbecco's Modified Eagle Medium
DMSO	Dimethylsulfoxide
DNase	Deoxyribonuclease
EDTA	Ethylenediaminetetraacetic acid
EGF	Epidermal growth factor
EHEC	Enterohemorrhagic *Escherichia coli*
FBS	Fetal bovine serum
FITC	Fluorescein isothiocyanate
GbpA	GlcNac-binding protein
GFP	Green fluorescent protein
GlcNac	N-Acetylglucosamine
GM1	Monosialotetrahexosylganglioside
HBSS	Hank's Balanced Salt Solution
HEPES	(4-(2-hydroxyethyl)-1piperazineethanesulfonic acid)
H_2O	water
HRP	Horseradish peroxidase
HRV	Human rotavirus
IPTG	Isopropyl-beta-D-thiogalactoside
Kan	Kanamycin
Kd	Kilodalton
LB	Luria Broth
Lgr5	Leucine-rich repeat-containing G-protein coupled receptor 5
LuxO	Luminescence regulatory protein O
M	Molar
Mam7	Multivalent adhesion molecule 7
MCM	Medium for making conditioned media
mg	Milligram
ml	Milliliter

mM	Millimolar
MSHA	Mannose-sensitive hemagglutinin
Muc2	Mucin-2
nm	Nanometer
ng	Nanogram
OD	Optical density
OmpU	Outer membrane protein U
PBS	Phosphate-buffered saline
PFA	Paraformaldehyde
PGE_2	Prostaglandin E_2
PSA	Penicillin-streptomycin-amphotericin B
qPCR	Quantitative polymerase chain reaction
RNA	Ribonucleic acid
RT	Room temperature
SI	Sucrase isomaltase
SILAC	Stable isotope labeling with amino acids in cell culture
TCP	Toxin co-regulated pilus
TEER	Trans-epithelial electrical resistance
TMB	Tetramethylbenzidine
UV	Ultraviolet
VC	*Vibrio cholerae*
WT	Wild-type
ZO-1	Zonula occludens 1
2D	Two-dimensional
3D	Three-dimensional
µg	Microgram
µl	Microliter
µM	Micromolar

Chapter 1: Introduction

1.1. *Vibrio cholerae* infection

Cholera, the disease caused by the Gram-negative bacterium *Vibrio cholerae* (VC), remains a major health problem in developing countries with inadequate water treatment and poor sanitation. The World Health Organization estimates that there are 1.3 to 4 million cases of cholera annually. A person can become infected with *V. cholerae* after ingesting contaminated water. Inside the host, *V. cholerae* travels to the small intestine and colonizes the distal section, the ileum. Once there, *V. cholerae* produces cholera toxin (CTX), its main virulence factor, which is largely responsible for the watery diarrheal symptoms. Cholera toxin subunit B binds to GM1 ganglioside receptors on the apical surface of intestinal epithelial cells and cholera toxin subunit A enters the cell [1]. Inside the cell, cholera toxin subunit A leads to ADP-ribosylation of GαS protein, which activates adenylate cyclase constitutively and leads to increased levels of cyclic AMP [2]. Protein kinase A is over-activated by the increased cyclic AMP levels and thus over-phosphorylates the cystic fibrosis transmembrane conductance regulator (CFTR) channel, which leads to massive chloride ion efflux. To maintain homeostatic ion balance, sodium ions and water also enter the intestinal lumen and exit the body, resulting in the characteristic rice-water diarrhea. Treatment with oral rehydration solution is usually effective. While cholera lethality rates have decreased over the past several decades, the number of cases has spiked in recent years [3].

1.2. Host physiology of the small intestine

The human small intestine functions to digest and absorb nutrients passing through the gastrointestinal tract. There are three sections of the small intestine, the duodenum, jejunum and ileum. The duodenum is closest to the stomach and the ileum is closest to the large intestine. The small intestine consists of a monolayer of epithelial cells that have a crypt-villus architecture. Below is a layer of mesenchymal cells and the vasculature, and above is a secreted mucus layer and microbiota that are in contact with the intestinal lumen. Various paracellular junctions are important for limiting movement from the intestinal lumen to the basolateral side of the epithelial cells. Two of these are tight junctions, which can be found at the apical side of the monolayer, and adherens junctions, which are more central [4].

The crypt-villus axis is a key structure that is maintained by chemical gradients. In the bottom of the crypts, there are $Lgr5^{+}$ stem cells and Paneth cells interspersed. Stem cells proliferate indefinitely and give rise to four types of differentiated cells. Stem cells are maintained by a Wnt3a signaling gradient and an inverse BMP signaling gradient [5]. Paneth cells produce lysozyme, an antimicrobial enzyme, which plays a role in innate immunity [4]. Along the axis, intermediary transit-amplifying cells grow and eventually give rise to differentiated cells. These differentiated cells include enterocytes, goblet cells, enteroendocrine cells, and the Paneth cells. Over time, enterocytes, goblet cells and enteroendocrine cells move towards the villus and are eventually recycled. Goblet cells secrete mucin which creates the mucus barrier between the epithelial cells and the intestinal lumen. Interestingly, CTX induces goblet cells to secrete mucin, even depleting goblet cells of their mucin reserves [4], [6]. Enteroendocrine cells are involved in

hormone peptide signaling. Enterocytes are the most abundant cell type and are responsible for nutrient absorption.

1.3. *V. cholerae* colonization

Although *V. cholerae* has been studied for over a century, uncertainty about the dynamics of *V. cholerae* colonization remains [7], [8]. Using an infant mouse model, it was shown that *V. cholerae* preferentially colonizes the crypts of the ileum [6], [9]. *V. cholerae* is able to penetrate the mucus layer and associate with the epithelial cells [7]. It is thought that *V. cholerae* must attach to the intestinal epithelium to cause disease, yet no specific attachment factor has been identified [7], [10]. The most studied colonization factor is the type IV toxin co-regulated pilus (TCP). TCP is required for colonization in the infant mouse model as well as in human volunteers [11], [12]. While many experiments have confirmed that it plays an important role in colonization, a clear mechanism has not been elucidated [10], [12], [13]. There is no evidence that this pilus directly attaches to epithelial cells and an epithelial receptor for TCP has not been identified [14]. It is currently thought that TCP allows bacteria to form microcolonies, which facilitates colonization [7], [12]–[14]. Microcolonies may provide protection from antimicrobials present in the intestine and promote favorable group behaviors [7]. For example, *V. cholerae* in microcolonies in the crypts may be protected from lysozyme released by crypt-based Paneth cells.

Further, it is thought that TCP is produced later in the infection process and other factors are important for initial attachment [7]. Less is known about how *V. cholerae* initiates attachment to intestinal epithelial cells. Several non-specific adhesins, including GlcNAc-binding protein (GbpA), multivalent adhesion molecule 7 (Mam7), outer

membrane protein OmpU, and the flagellum have all been implicated in the initial attachment process using various animal and cell culture models [7], [9], [15], [16], [17].

Initial attachment is hypothesized to be reversible or noncommittal until *V. cholerae* reaches a favorable niche [7]. In support of this, it is known that motility is an important colonization factor in the duodenum, but not in the ileum [9]. Perhaps this is because the ileum is the preferred colonization environment, so once the bacteria have reached this niche, motility is no longer important. Neither motility nor chemotaxis were found to be important for localization along the crypt-villus axis [9].

1.4. *V. cholerae* damage to host tight junctions

As mentioned above, cholera toxin is the main virulence factor of *V. cholerae*. CTX upregulates cyclic AMP production inside the host cell and triggers chloride ion efflux via the CFTR channel and subsequent sodium ion and water efflux, most likely from a paracellular route. Thus, it has been hypothesized that CTX damages paracellular junctions, which could explain how this massive sodium ion and water loss occurs. The suggested mechanism is that elevated cyclic AMP levels inhibit Rab11-mediated trafficking of host junction proteins to cell borders. Guichard et al. studied the effect of purified CTX on Caco-2 cell tight junctions. Cells were treated 3 times every 12 hours with 100 ng/ml CTX at each time point and tight junctions were observed using an antibody against the protein Zonula Occludens 1 (ZO-1) [18]. They observed that tight junctions treated with CTX became meandering paths and ZO-1 protein seemed to mislocalize and accumulate above nuclei [18]. Further, some tight junctions no longer aligned with lower adherens junctions [18]. However, they did not show if tight junction integrity and barrier function were impaired in this study. In another study,

Sawasvirojwong et al., looked for damage caused to tight junctions by WT *V. cholerae*. They inoculated adult ligated mouse ileal loops with 10^7 CFU WT *V. cholerae* and observed intestinal fluid secretion 12 hours post infection. To determine if paracellular junction damage was the cause of this fluid secretion, they measured the trans-epithelial electrical resistance (TEER) and performed a permeability assay using FITC-dextran molecules [19]. After infection with *V. cholerae* or intoxication with CTX, intestinal fluid was removed from the ligated ileal loops and FITC-dextran molecules were added back to the lumen. The animals were sacrificed thirty minutes post-treatment, and FITC-dextran present in the blood was measured to indicate intestinal paracellular permeability. There was no difference found in either assay when CTX-treated samples were compared to saline-treated control samples [19]. As will be discussed below, adult mice are not naturally colonized by *V. cholerae* and even though the effects of CTX were observed in this ligated ileal loop system, it remains unclear if *V. cholerae* causes damage to paracellular tight junctions during normal infection.

1.5. Current models used to study *V. cholerae*

Small animal and cell culture models are routinely used to study *V. cholerae* host-pathogen interactions. Studies using these models have led to many findings and a deepened understanding of *V. cholerae* pathogenesis. However, the available model systems have distinct limitations [20]. As cholera remains a global health problem today without an efficient preventative scheme other than better sanitation, there is a need to develop alternative models to fill gaps in knowledge.

1.5.1. Infant mouse model

V. cholerae does not normally colonize adult mammals except humans, thus infant animal models are usually used to study this pathogen [21]. The infant mouse model is the most commonly used animal model to study *V. cholerae* [10], [13], [21]. Infant mice were validated as a model when results replicated those from human volunteer studies; TCP and ToxR, a virulence regulator, are required for intestinal colonization in both humans and infant mice [12], [13]. These findings suggest that this model is relevant to human infection. It incorporates mechanical aspects of the intestine, including peristalsis and digestion, that *in vitro* models lack [10], [20].

Yet, the usefulness of this model is limited. Importantly, mice do not experience symptomatic cholera as humans do. Suckling mice become resistant to *V. cholerae* infections when they are 10 days old. Thus, it is challenging to study factors that are important in causing damage to host tissues and are responsible for the characteristic rice-water diarrhea [13]. It was also found that motility genes are not required for infant mouse intestinal colonization, while these factors are required for infections in infant rabbits and human volunteers [21]. Moreover, this model cannot be used for vaccine studies, because "suckling mice are separated from their mothers and do not survive long enough to acquire protective immunity" [21].

1.5.2. Infant rabbit model

Infant rabbits are an important model for studying *V. cholerae* because unlike infant mice, rabbits experience the watery diarrheal symptoms. This difference can likely be attributed to negligible intestinal flora in infant rabbits [13]. This model has been deemed useful for studying *V. cholerae* colonization and enterotoxicity [22]. TCP is required for

infant rabbit intestinal colonization and CTX is required for diarrhea to present as a symptom [6], [22].

However, infant rabbits are more expensive than infant mice. This and availability of litters limit experiment size. It is key that all rabbits are of a very similar age, and that they are young, because similarly to mice, adult rabbits are naturally resistant to infection with *V. cholerae* [22]. It has also been noted that significant variability exists between different litters, and that this can affect the "kinetics of disease progression" [22]. There are also several disadvantages from a practical standpoint. Adult females may reject litters that have been handled by humans, infant rabbits can be challenging to handle, and "an experiment is entirely dependent on the delivery date of infant rabbits" [22].

1.5.3. General disadvantages of animal models

Primarily, animal models are used to study the events that happen at a later stage of infection, usually around 12-48 hours-post-infection. Thus, initial attachment, colonization, and early virulence mechanisms are often overlooked. In the infant mouse model, Millet et al. could not detect any bacteria 8 hours-post-infection with confocal microscopy and it was assumed that most *V. cholerae* had not attached yet [9]. No microcolonies had formed and only small ones were visualized by 16 hours-post-infection [9].

Moreover, it is challenging to study the "zoomed-in" interactions that occur between *V. cholerae* and the small intestinal epithelial surface with these animal models. Researchers are limited to certain types of experiments, most commonly ones that compare input and output [21]. Other available animal models, including chinchillas,

guinea pigs, zebrafish, and fruit flies all have significant limitations and thus are not commonly used [22].

1.5.4. *in vitro* Caco-2 cell culture model

Caco-2 cells are a human epithelial cell line derived from colon adenocarcinoma and can form a polarized monolayer with a villous apical side and a basolateral side. This cell culture system permits studies that would be challenging to do in animal models, such as studying very early time points in the course of infection and looking closely at host cell damage. Caco-2 cells have been used to study adherence of non-O1 *V. cholerae* strains and subsequent damage caused to microvilli [23]. Other examples of how this model has been used include studying the effect of CTX, determining the protective effects of synthetic peptides that block CTX attachment to GM1 receptor, assessing adherence and the role of microbiota competition, and confirming host cell gene expression regulation observed in patient samples [18], [24]–[26]. Another advantage of the Caco-2 cell culture system is that it can be used for higher throughput screening experiments than animal models.

However, the Caco-2 cell model has several disadvantages. First, as mentioned, they are derived from a cancerous cell line, which indicates that there are unknown mutations and that the cells may not behave as normal intestinal cells [27]. Additionally, they do not produce a mucus layer and only represent one particular cell type. Further, *V. cholerae* primarily infects the ileum of the small intestine, not the colon. In sum, there is not a single perfect model for studying *V. cholerae*. There is an urgent need for an alternative to the existing models, so that the early infection processes and initial attachment dynamics of *V. cholerae* can be studied in a relevant setting.

1.6. Enteroids

Organoids are mini 3D self-organizing structures derived from their respective organ tissue. Enteroids are organoids that are derived from a biopsy of the small intestine, from the duodenum, the jejunum, or the ileum. The ileum is the most distal section from the stomach. Sato and Clevers first developed a reliable and reproducible system to isolate stem cells from the crypts of a human small intestinal biopsy that could be cultured indefinitely and made to differentiate into multiple cell types [28]. Enteroids are a promising new model as they provide several advantages over simple cell culture models. Unlike Caco-2 cells, they are non-cancerous and thus physiologically more representative than immortal cell lines. Enteroids can be differentiated into multiple cell types, thereby mimicking the cell composition of the intestinal epithelial layer. Gastrointestinal epithelial cell biology, gene expression, and function are largely recapitulated by enteroids cultured *ex vivo* [27].

1.6.1. Enteroid physiology and differentiation

Enteroids are small intestinal stem cells that can be maintained in culture indefinitely. Enteroids in their stem cell state are cultured in the presence of several important signaling factors including Wnt3a, R-Spondin-1, Noggin, and other factors that promote stem cell state and long-term viability. Upon removal of primarily Wnt3a and R-Spondin-1, enteroids differentiate into the 3 major small intestinal cells: enterocytes, Goblet cells, and enteroendocrine cells [29]. The 4^{th} major cell type, Paneth cells, are present before removal of these factors from the medium [5]. Like in the small intestine, enterocytes comprise the majority of cells present. Presence of all four cell types have been confirmed in duodenal and jejunal enteroids by immunofluorescence, and jejunal

enteroids by qPCR [30], [31]. When split into a single-cell state, enteroids are able to form a monolayer and polarize with an apical brush border of microvilli.

3D enteroids are clear and cystic or multi-lobulated in appearance [30]–[32]. They are maintained in Matrigel, a substance that mimics the extracellular matrix. The Matrigel dome is submerged in media composed primarily of conditioned media harvested from cell lines over-producing Wnt3a, R-Spondin-1, and Noggin. Enteroids naturally exist in a state where the apical side of the epithelium faces the interior lumen and the basolateral side is exposed to the Matrigel and media**.** Recently, Co et al. developed a method for inverting 3D enteroids so that the apical surface faces exteriorly [33]. This is an important development because as they demonstrated, 3D enteroids can be better used for host-pathogen studies, as most pathogens come into contact with the apical surface first.

1.6.2. Current applications of enteroids

It has been suggested that enteroids have many potential applications. Enteroids from patients with different traits can be collected and stored as biobanks. For example, enteroids can be obtained from individual donors with different age groups or biological sexes, or who have different blood types or disease states. This is a unique aspect of this cell culture model and will allow for many novel studies. Enteroids can also be used for high-throughput drug screening, gene editing therapies, and omics profiling [34]. As many as 90% of human drug studies based on animal and simple cell line research fail [29]. As enteroids and other organoids are derived from human tissue, failures due to unexpected toxicity or inefficacy could be avoided.

1.6.3. Enteroids as models of host-pathogen interactions

Enteroids have been used to study intestinal diarrheal diseases, including human rotavirus (HRV), enterohemorrhagic *Escherichia coli* (EHEC), norovirus, and salmonella [29], [35]. Previously, it was very difficult to study human rotavirus because it replicates poorly in transformed cell lines and animal models [30]. Saxena et al. found that HRV is able to infect enteroids, preferentially targeting differentiated enterocytes and enteroendocrine cells [30]. Similarly, Ettayebi et al. cultured noroviruses in enteroids, which also previously did not have an established model [36]. Foulke-Abel et al. infected enteroids with EHEC and observed actin cytoskeletal changes that resembled micropinocytosis, which is known to occur in the small intestine [29]. Two groups have recently developed enteroids as models for studying *Shigella flexneri* [37], [38]. Both groups found that *S. flexneri* seems to preferentially invade monolayers from the basolateral surface. Ranganathan et al. found that *S. flexneri* induced higher expression levels of Mucin-2 [37]. Co et al. found that *Salmonella enterica* infects the apical side of 3D inverted enteroids (apical side out) more efficiently than the basolateral side, and that *Listeria monocytogenes* targets sites of cell extrusion [33]. Kuhlmann et al. studied the effect of cholera toxin on enteroids derived from patients with different blood types [39]. Epidemiological data suggests that individuals with blood type O are more susceptible to severe cholera [39], [40]. Blood type O enteroids treated with CTX had higher levels of cyclic AMP when compared to blood type A-enteroids [39]. Thus, there has been success in developing enteroids to study host pathogen interactions. As any model, there are some limitations. While enteroids are a more robust model than Caco-2 cells, they still lack

physiological features like immune cells, mesenchymal cells, a microbiome, peristalsis, digestion, and intestinal flow.

Chapter 2: Materials and Methods

2.1. Bacterial strains

All *V. cholerae* strains used in this study are El Tor biotype, C6706str2. Δ*luxO V. cholerae* has been previously described [41]. Δ*tcpA V. cholerae* was constructed by mating an *E. coli* SM10λpir (pHT3) strain with an in-frame *tcpA* deletion construct, originally from Thelin, Taylor 1996, with our lab C6706 strain [11]. All strains used in this study carry an IPTG-inducible plasmid, pEVS143-GFP with kanamycin resistance.

2.2. Caco-2 Cells

2.2.1. Caco-2 Cell Maintenance

Caco-2 cells were grown in Dulbecco's Modified Eagle Medium (DMEM) supplemented with 10% Fetal Bovine Serum (FBS) and 1% penicillin-streptomycin-amphotericin B (PSA). Cells were maintained in tissue culture flasks in 15 ml of this media in a sterile tissue culture incubator at 37C with 5% CO_2. To passage cells, spent media was removed and cells were washed with 10 ml phosphate-buffered saline (PBS). Trypsin-EDTA (1.5 ml) was added at 37C until cells begin to detach from flask. To fully detach cells, 8.5 ml of fresh media was added and pipetted against the back of the flask. Two ml of the suspension were transferred to a new culture flask containing 13 ml of fresh media (1:5 split).

2.2.2. Caco-2 Cell Monolayer Preparation

Sterile 24-well transwells (ThinCert™ Tissue Culture Inserts, Greiner Bio-One 662641) were coated with 50 μg/ml Collagen 1 (Rat Protein, Tail) diluted in 60% ethyl alcohol and exposed to UV light in a sterile tissue culture hood overnight. To seed transwells with Caco-2 cells, normal passaging protocol was followed. Instead of seeding cells into

a new culture flask, all 10 ml was transferred to a 50 ml conical tube and mixed well. Ten µl of suspended cells were counted with a hemocytometer and the volume needed was calculated for 3.5E4 cells/transwell. Suspended cells were then diluted in DMEM supplemented with 10% FBS and 1% PSA to 1.166E5 cells/ml and 300 µl of the suspension was added to the apical side of each transwell and 900 µl of fresh media to the basolateral side. The next day, apical media was removed and replaced with DMEM with 1% PSA only (no FBS). Media was refreshed every other day for 14-21 days to allow cells to polarize. TEER was occasionally measured to ensure that monolayers were forming properly and becoming confluent. The day before infection, apical and basolateral media were replaced with antibiotic-free media.

2.3. Enteroids

2.3.1. Enteroids Maintenance

Enteroid maintenance and passaging protocols were developed and previously described by Sato et al. 2011 [28]. Enteroids are maintained in a dome of Corning® Matrigel® Matrix, which mimics extracellular matrix. Ideal Matrigel® protein concentration is 8.5-9.0 mg/ml. Each Matrigel® dome is submerged in 500 µl of conditioned media plus growth factors ($CMGF^+$) per well, in 24-well cell culture plates (Olympus Plastics, 25-107). First, $CMGF^-$ was prepared by mixing 500 ml advanced DMEM/F12, 5 ml GlutaMAX-I, and 5 ml HEPES. Then, 20 ml of $CMGF^+$ was prepared by mixing 1.5 ml $CMGF^-$, 15 ml Wnt3a conditioned medium, 2 ml R-Spondin conditioned medium, 1 ml Noggin conditioned medium, 200 µl B27 supplement, 100 µl N2 supplement, 20 µl N-acetylcysteine, 10 µl EGF, 10 µl [Leu15]-Gastrin I, 100 µl nicotinamide, 10 µl A-83-0,

and 10 μl SB202190. $CMGF^+$ is prepared weekly or more frequently. The components of this media are described in detail in the following table.

Reagent	Supplier	Cat No.	Solvent	[Stock]	[Final]
GlutaMAX-I	Invitrogen	35050-061	-	200 mM	2 mM
N2 supplement	Invitrogen	17502-048	-	100x	1x
B27 supplement	Invitrogen	17504-044	-	50x	1x
N-Acetylcysteine	Sigma-Aldrich	A9165	ddH_2O	500 mM	1 mM
Mouse recombinant EGF	Invitrogen	PMG8043	PBS	500 μg/ml	50 ng/ml
A-83-01	Tocris	2939	DMSO	500 μM	500 nM
SB202190	Sigma-Aldrich	S7067	DMSO	30 mM	10 μM
Nicotinamide	Sigma-Aldrich	N0636	ddH_2O	1M	10 mM
[Leu15]-Gastrin I	Sigma-Aldrich	G9145	PBS	100 μM	10 mM
HEPES 1M	Invitrogen	15630-080	-	1M	10 mM
Advanced DMEM/F12	Invitrogen	12634-028	-	-	-
Mouse recombinant Wnt3a	ATCC	CRL-2647	-	10 μg/ml	100 ng/ml
Human recombinant R-Spondin	Trevigen	3710-001-K	-	1 mg/ml	1 μg/ml
Mouse recombinant Noggin	Van den Brink	-	-	100 μg/ml	100 ng/ml

Table 2. 1. Components of $CMGF^+$ required for enteroid growth

Adapted with permission from T. Sato et al., "Long-term Expansion of Epithelial Organoids From Human Colon, Adenoma, Adenocarcinoma, and Barrett's Epithelium," Gastroenterology, vol. 141, no. 5, pp. 1762–1772, Nov. 2011. Changes include table organization, different sources for human recombinant R-Spondin, mouse recombinant Wnt3a, and mouse recombinant Noggin, removal of factors from the table including Matrigel, Penicillin/Streptomycin, EDTA, human recombinant FGF10, Y-27632, and DNase.

2.3.2. Conditioned Media Preparation

Conditioned media harvested from three different cell lines over-producing Wnt3a, R-Spondin, and Noggin are required for enteroid $CMGF^+$. Conditioned medium from each cell line was prepared as previously described in conditioned media protocols [32]. All cultures are incubated at 37C with 5% CO_2.

2.3.2.1. Wnt3a Conditioned Medium Protocol

To make Wnt3a growth medium, advanced DMEM was supplemented with 10% FBS and 0.4 mg/ml Geneticin™ Selective Antibiotic (G418 Sulfate, Thermo Fisher 10131-035). Wnt3a cells from frozen stock were cultured in Wnt3a growth medium. When confluent, cells were split with trypsin-EDTA 1:10 into 10 new culture flasks. One flask was maintained in 15 ml Wnt3a growth medium for passaging. The other 9 flasks were maintained in 10 ml medium for making conditioned media (MCM). MCM is advanced DMEM supplemented with 10% FBS and 1:100 GlutaMAX. The 9 flasks were cultured for 4 days and medium was harvested, centrifuged at 1000g and sterile filtered (0.22 μM filter). Ten ml of fresh MCM was added to each flask and cultured for 3 more days. Medium was harvested, centrifuged at 1000g and sterile filtered. The two batches of media were combined and stored short-term at -20C or long-term at -80C until ready for use.

2.3.2.2. R-Spondin Conditioned Medium Protocol

To make R-Spondin growth medium, advanced DMEM was supplemented with 10% FBS and 300 μg/ml Zeocin™ Selection Reagent (Invitrogen R25001). R-Spondin cells from frozen stock were cultured in R-Spondin growth medium until 80% confluent. Cells were split with trypsin-EDTA 1:5 into 5 new flasks. One flask was maintained in 15 ml R-Spondin growth medium for passaging. The other 4 flasks were maintained in 15 ml of MCM. When 80% confluent, cells were treated with trypsin-EDTA diluted 1:3 in PBS at room temperature very briefly. Trypsin was inactivated by addition of 8.5 ml DMEM supplemented with 10% FBS. Medium was pooled in a 50 ml conical tube and centrifuged at 200g for 5 minutes. Supernatant was removed and pellet of cells was

divided into 10 new culture flasks with 20 ml MCM each. Cells were cultured for 7 days, medium was harvested, centrifuged at 1000g for 10 minutes, and sterile filtered (0.22 μM filter). Medium was stored short-term at -20C or long-term at -80C until ready for use.

2.3.2.3. Noggin Conditioned Medium Protocol

To make Noggin growth medium, advanced DMEM was supplemented with 10% FBS and 10 μg/ml puromycin dihydrochloride (Invitrogen A11138-02). Noggin cells from frozen stock were cultured in Noggin growth medium until 80% confluent. Cells were split with trypsin-EDTA 1:5 into 5 new flasks. One flask was maintained in 15 ml Noggin growth medium for passaging. The other 4 flasks were maintained in 15 ml of MCM. When 80% confluent, cells were treated with trypsin-EDTA diluted 1:3 in PBS at room temperature very briefly. Trypsin was inactivated by addition of 8.5 ml DMEM supplemented with 10% FBS. Medium was pooled in a 50 ml conical tube and centrifuged at 200g for 5 minutes. Supernatant was removed and pellet of cells was divided into 10 new culture flasks with 20 ml MCM each. Cells were cultured for 7 days, medium was harvested, centrifuged at 1000g for 10 minutes, and sterile filtered (0.22 μM filter). Medium was stored short-term at -20C or long-term at -80C until ready for use.

2.3.3. Passaging Enteroids

This protocol has been adapted from those previously described [28], [32]. Enteroids are usually passaged every 7 days. Before beginning, the needed amount of Matrigel® was thawed on ice for 1-2 hours. Alternatively, Matrigel® can be thawed quickly at room temperature (RT) and kept on ice for immediate use, without gelling. Both methods worked, and no morphological differences were observed between them. To passage, media was removed from wells and 500 μl of cold $CMGF^-$ was added to each well. To

thoroughly mechanically disrupt the Matrigel® dome, the pipette tip was scraped against the bottom of the well and medium was pipetted up and down several times. Then, a 1 ml syringe with a 25G x 5/8 needle was used to pipette contents of the well up and down, once back into the well and a second time into a 15 ml conical tube. Multiple wells (often 6 wells) were combined in one 15 ml tube. 2x cold $CMGF^-$ was added to the 15 ml conical tube (for 6 wells of 500 µl each (3 ml), 6 ml of cold CMGF- was added). Conical tubes were centrifuged at 80g at 4C for 6 minutes (in a refrigerated swing rotor centrifuge). After centrifugation, media was removed and tubes were placed on ice. Working quickly and with one 15 ml tube at a time, enteroid pellets were resuspended in Matrigel® and pipetted as 30 µl droplets into the center of individual wells, being careful to avoid any bubbles in the Matrigel®. To allow Matrigel® to solidify correctly, 24-well plates were quickly and carefully inverted and placed into a sterile tissue culture incubator at 37C with 5% CO_2 for 10-15 minutes. These steps were repeated for all conical tubes while plates incubated. After incubation, 500 µl of warm $CMGF^+$ was added to each well and incubated. $CMGF^+$ media was changed every other day (3-4 times between passages).

2.3.4. Enteroid Monolayer Preparation

This protocol was previously described by Zou et al. [32]. Sterile 24-well transwells were coated with 100 µl of 33 µg/ml Collagen IV (Sigma C5533) diluted from stock solution of 1 mg/ml in 100 mM acetic acid in cold H_2O. Transwells were incubated at 37C with 5% CO_2 for 2-3 hours. Enteroids for seeding transwells were removed from Matrigel® by adding 500 µl of cold 0.5 mM EDTA (0.5 M EDTA diluted in PBS) and mechanically disrupting with the pipette tip. Enteroids in Matrigel® were centrifuged for 5 minutes at

300g at 4C (in a refrigerated swing rotor centrifuge). Medium was removed and the enteroid pellet was treated with 500 µl (pellets from 2-5 wells) or 1 ml (pellets from 6-12 wells) of 0.05% trypsin-0.5 mM EDTA at 37C for 4 minutes. Trypsin was immediately inactivated by adding 1 ml of warm $CMGF^-$ supplemented with 10% FBS. Enteroids were vigorously pipetted up and down at least 50 times to ensure dissociation. Then, dissociated enteroids were passed through a 40 µm cell strainer pre-wet with 1 ml of $CMGF^-$ supplemented with 10% FBS. 10 µl of strained cells were counted with a hemocytometer and calculated for 2.5E5 cells/transwell or 2.5E6 cells/ml for 100 µl/transwell. Cells that passed through strainer were pelleted for 6 minutes at 400g at 4C (in a refrigerated swing rotor centrifuge) and the enteroid pellet was resuspended in the calculated amount of transwell medium, which is $CMGF^+$ medium without nicotinamide or SB202190 and supplemented with 10 µM Y-27632 (Sigma Y-0503) to prevent apoptosis. Remaining collagen solution was removed from transwells and 100 µl of resuspended enteroids was added to the apical side of each transwell. 600 µl of transwell medium was added to the basolateral side. Two days-post-seeding, apical and basolateral media were replaced with 150 µl and 600 µl differentiation medium, respectively. 10 ml of differentiation medium was prepared by mixing 9.15 ml of $CMGF^-$, 500 µl Noggin conditioned medium, 200 µl B27 supplement, 100 µl N2 supplement, 20 µl N-acetylcysteine, 10 µl EGF, 10 µl [Leu15]-Gastrin I, and 10 µl A-83-0. Enteroid monolayers were used for experiments 7 days-post-seeding (which is 5 days-post-differentiation). Media was changed every other day and transwells were concurrently relocated to a new 24-well plate.

2.4. Monolayer Infection (Caco-2 Cells and Enteroids)

V. cholerae cultures were grown in Luria Broth (LB) with 100 μg/ml kanamycin and 100mM IPTG overnight at 37C. The next day, OD_{600} was measured and cultures were back-diluted to ~5E6 CFU/ml (1 OD_{600} was pre-determined to be 1E9 CFU/ml), unless otherwise stated. Two hundred μl of the diluted culture (1E6 CFU/transwell) was added to the apical side of each transwell and allowed to incubate in a tissue culture incubator at 37C with 5% CO_2 for a specified amount of time. In some cases, as specified in the results, infected medium was removed 45-minutes post-infection and replaced with fresh medium. At the final time point, infected medium was removed and monolayers were washed once with fresh medium or PBS. For all Caco-2 cell monolayer infections, apical medium was DMEM and basolateral medium was DMEM supplemented with 10% FBS. For enteroid monolayer infections, apical medium was PBS, unless otherwise specified in the results, and basolateral medium was always 600 μl of enteroid differentiation medium. For CFU enumeration, monolayers were treated with 300 μl of 1% Triton X-100 in PBS for 15 minutes at RT on a rocker. Each sample was transferred to an Eppendorf tube containing 200 μl of LB, vortexed and pipetted to disrupt bacterial clumps. Samples were serially diluted and 10 μl of selected dilutions were plated on LB-Kan plates and incubated overnight at 37C. For analysis by confocal immunofluorescence microscopy, transwells were placed into a new 24-well plate with 900 μl of fresh PBS on the basolateral side. Monolayers were treated with 100 μl of 4% paraformaldehyde (PFA) and incubated for 25 minutes at RT in the dark. Monolayers were washed three times with 300 μl PBS and stored at 4C wrapped in tinfoil with 300 μl of fresh PBS on the apical side.

2.5. Immunofluorescence Staining and Confocal Microscopy

2.5.1. Immunofluorescence Antibodies and Probes

Primary antibodies that were used (at specified dilutions) include mouse monoclonal anti-Zonula Occludens 1 (ZO-1) (1:50), mouse monoclonal anti mucin-2 (Muc2) (1:100), mouse monoclonal anti-sucrase isomaltase (SI) (1:100), rabbit monoclonal anti-lysozyme (Lys) (1:100), and rabbit polyclonal anti-chromogranin A (ChgA) (1:100). Secondary antibodies that were used include goat anti-mouse Alexa Fluor 594 (1:200) and goat anti-rabbit Alexa Fluor 514 (1:100). Probes that were used include Alexa Fluor™ 647 Phalloidin (1:100) for actin labeling and DAPI (1:100) for nucleic acid staining.

2.5.2. Immunostaining Transwell Monolayers

After being fixed with 4% PFA and washed with PBS, monolayers were permeabilized with 100 µl of 1% Bovine Serum Albumin (BSA) with 0.1% Triton X-100 for 5 minutes in the dark at RT. Monolayers were washed 3 times with 300 µl PBS. One hundred µl of solution containing primary antibody in 1% BSA with 0.1% Triton X-100 was added per transwell for 1 hour in the dark at RT. Monolayers were washed 3 times with 300 µl PBS. One hundred µl of solution containing secondary antibodies and probes in 1% BSA with 0.1% Triton X-100 was added per transwell for 30 minutes in the dark at RT. Monolayers were washed a final 3 times with 300 µl PBS. The monolayer attached to the membrane of the transwell was cut out, placed on a microscope slide (with the side of the membrane with cells facing up) with a drop of ProLong® Gold Antifade Mountant, and covered with a coverslip. Microscope slides were allowed to dry overnight in the dark at room temperature.

2.5.3. Confocal Microscopy

Images of monolayers were obtained with a Nikon A1R inverted confocal microscope. Oil lenses at 40x or 60x magnification were used. Z-stack images were taken with high resolution (1024) and 2x average per slice. Step size was 0.5 μm. Most images were taken at 40x magnification; it is stated if they were taken at 60x magnification.

2.5.4. Analysis by Fiji/ImageJ

Fiji-ImageJ software was used to analyze confocal microscopy data. Maximum intensity Z-stack projections were obtained and quantified by using the ImageJ Object Count function or by setting a threshold and measuring the percent area fluorescent. All scale bars are 20 μm unless otherwise specified.

2.6. Quantitative Polymerase Chain Reaction (qPCR)

Enteroids in Matrigel® were disrupted with addition of 500 μl of cold $CMGF^-$, centrifuged in a tabletop centrifuge at 150-250g for 5 minutes, and treated with 1 ml of TRIzol. Enteroids seeded as monolayers were treated with 300 μl TRIzol, removed from transwell, and added to 700 μl TRIzol. RNA was isolated from samples, treated with DNase, cleaned and concentrated with a kit, synthesized into cDNA, and used for qPCR. Primers used are described in the table below. Primers for sucrase isomaltase and lysozyme were previously described by Chen et al. 2017 [42].

Gene	Forward Primer	Reverse Primer
GAPDH	ACCACAGTCCATGCCATCAC	TCCACCACCCTGTTGCTGTA
$Lgr5^+$	TCAGTCAGCTGCTCCCGAAT	CGTTTCCCGCAAGACGTAAC
Muc2	ATGCCCTTGCGTCCATAACA	AGGAGCAGTGTCCGTCAAAG
SI	TCCAGCTACTACTCGTGTGAC	CCCTCTGTTGGGAATTGTTCTG
Lys	CGCTACTGGTGTAATGATGG	TTTGCACAAGCTACAGCATC
Chga	GTCGGGGTATATAAGCGGGG	CGTCTGTCGGTCGATCCTC

Table 2. 2. Primers for qPCR of enteroids

Primers that were used to detect stem cells ($Lgr5^+$), goblet cells (Muc2), enterocytes (SI), Paneth cells (Lys), and enteroendocrine cells (Chga).

2.7. Monolayer tight junction integrity assay

The enzyme horseradish peroxidase (HRP) was used to determine tight junction integrity. Previously, this method was described by Chen and Yeh 2017 [43]. Briefly, 40 μL of streptavidin-HRP was added to 2.56 ml of Hank's Balanced Salt Solution $(HBSS)^{+}$. Transwells were placed into a new 24-well plate with 1ml of $HBSS^{+}$ per well (basolateral side). One hundred μl of the HRP solution was added to the apical side of the transwell prior to infection. Transwells were allowed to incubate at 37C with 5% CO_2 for 20 minutes. Twenty μl of media from the basolateral side of each transwell was plated in duplicate into a clear 96-well plate. Fifty μl of TMB substrate was added to each well and incubated at RT for 5 minutes. Twenty five μL of sulfuric acid was added to each well to stop reaction. Absorption reads (450 nm) were immediately acquired with a plate reader. This protocol was repeated after infection with *V. cholerae*.

Chapter 3: Validating Cell Culture Monolayers as a Model for *V. cholerae* Infection

Caco-2 cells have been recognized as an *in vitro* model for *V. cholerae* studies. Yet, they are used less frequently than *in vivo* mouse and rabbit models. Therefore, infection protocols for various systems, such as transwells, are not widely standardized. Here, 2D transwell infection parameters are optimized and phenotypes of a previously-characterized mutant strain, Δ*luxO V. cholerae,* are validated.

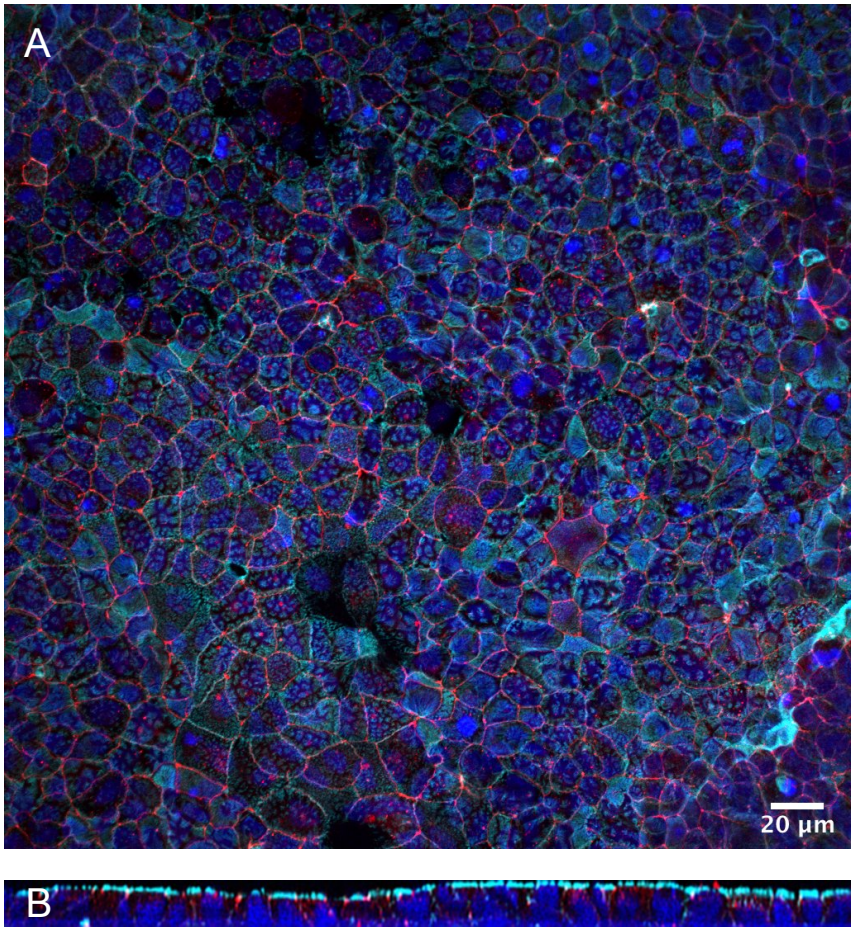

Figure 3. 1. Caco-2 cells form polarized monolayers

Confocal immunofluorescence microscopy Z-stack projection shows (A) Caco-2 cells form tight junctions, observed in red with ZO-1 antibody. Cross-sectional view shows (B) Caco-2 cells polarize with an apical brush border, observed in light blue with phalloidin stain. Nuclei are stained with DAPI and appear dark blue.

3.1. Optimization of 2D transwell monolayer system using Caco-2 cells

Many cell culture experiments are performed with cells seeded on a flat glass surface, such as a coverslip, submerged in media [44]. Seeding cells on a transwell adds a layer of complexity with separated apical and basolateral sides. This organization mimics the structure of the intestine, where the apical side is exposed to the intestinal lumen and the basolateral side to the underlying vasculature. Here, Caco-2 cells were seeded onto the apical side of collagen-coated transwells. Medium without FBS was added to the apical side and medium containing FBS was added to the basolateral side to allow monolayers to fully polarize for a minimum of 14 days and up to 21 days. Confocal immunofluorescence microscopy confirmed that Caco-2 cell transwell monolayers are confluent, polarize with an apical brush border, and form tight junctions (Figure 3.1). WT *V. cholerae* and all other strains in this study have an IPTG-inducible pEVS143-GFP

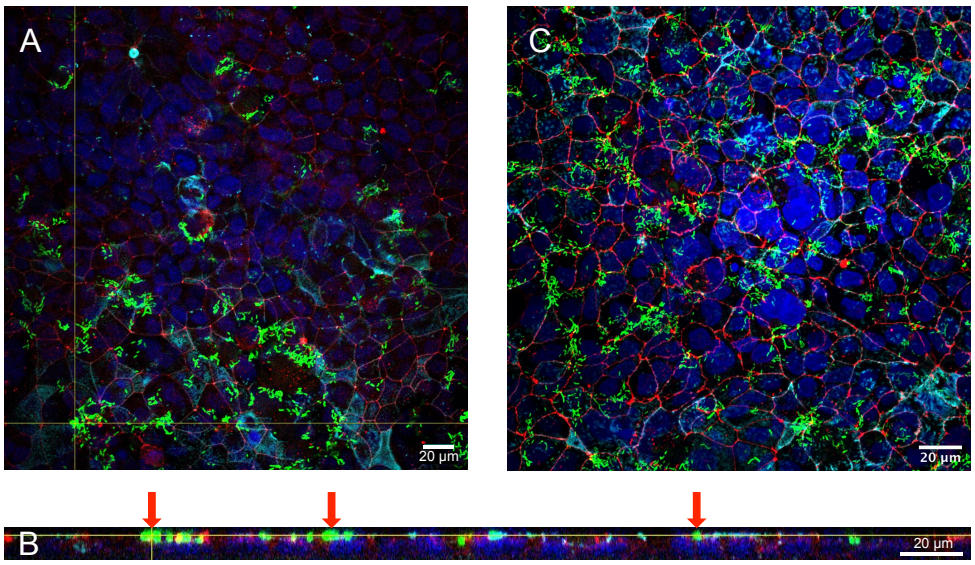

Figure 3. 2. *V. cholerae* associates with Caco-2 cell monolayer

Caco-2 cell monolayers were inoculated with 5.5E5 CFU WT *V. cholerae*. (A) Top view of one slice of Z-stack and (B) cross-sectional view show individual and clusters of *V. cholerae* associating 2 hours-post-infection. Red arrows denote associated bacteria (green). (C) 60x magnification maximum intensity Z-stack projection shows *V. cholerae* associated with the monolayer 3 hours post infection.

plasmid with kanamycin resistance and thus appear green in microscopy images. At 2 or 3 hours-post-infection, WT *V. cholerae* was found to associate with the apical surface of the monolayer in small clusters or as individual bacteria (Figure 3.2). In animal models, *V. cholerae* is known to form clonal microcolonies [10][4]. The initial inoculum was optimized so that data could be most accurately analyzed; if bacteria were too scarce or too abundant in the transwell it would make quantification challenging. Analysis by confocal microscopy determined that approximately 5.5E5 CFU to 1E6 CFU *V. cholerae*

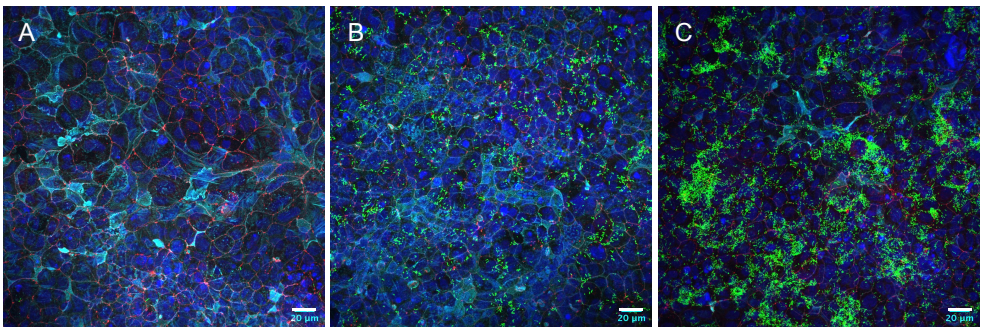

Figure 3. 3. 1E6 CFU *V. cholerae* is the optimal initial inoculum

Confocal immunofluorescence microscopy Z-stack projections of Caco-2 cell monolayers infected with (C) 1E5 CFU, (D) 1E6 CFU, or (E) 1E7 CFU WT *V. cholerae* for 1.5 hours. Red denotes tight junctions, green denotes *V. cholerae*, light blue denotes actin, and dark blue denotes nuclei.

is the optimal range for the initial inoculum (Figure 3.3). In this range, individual bacterial cells were clearly visible and could be more accurately quantified. To determine if bacteria are associating and growing in the presence of Caco-2 cell monolayers, monolayers were infected with 5.5E5 CFU *V. cholerae* for increasing incremental time points. As expected, *V. cholerae* associates with the monolayer increasingly over time (Figure 3.4). However, it is unclear from this experiment if *V. cholerae* are replicating on the Caco-2 cell monolayer or simply if more bacteria are associating over time from the supernatant.

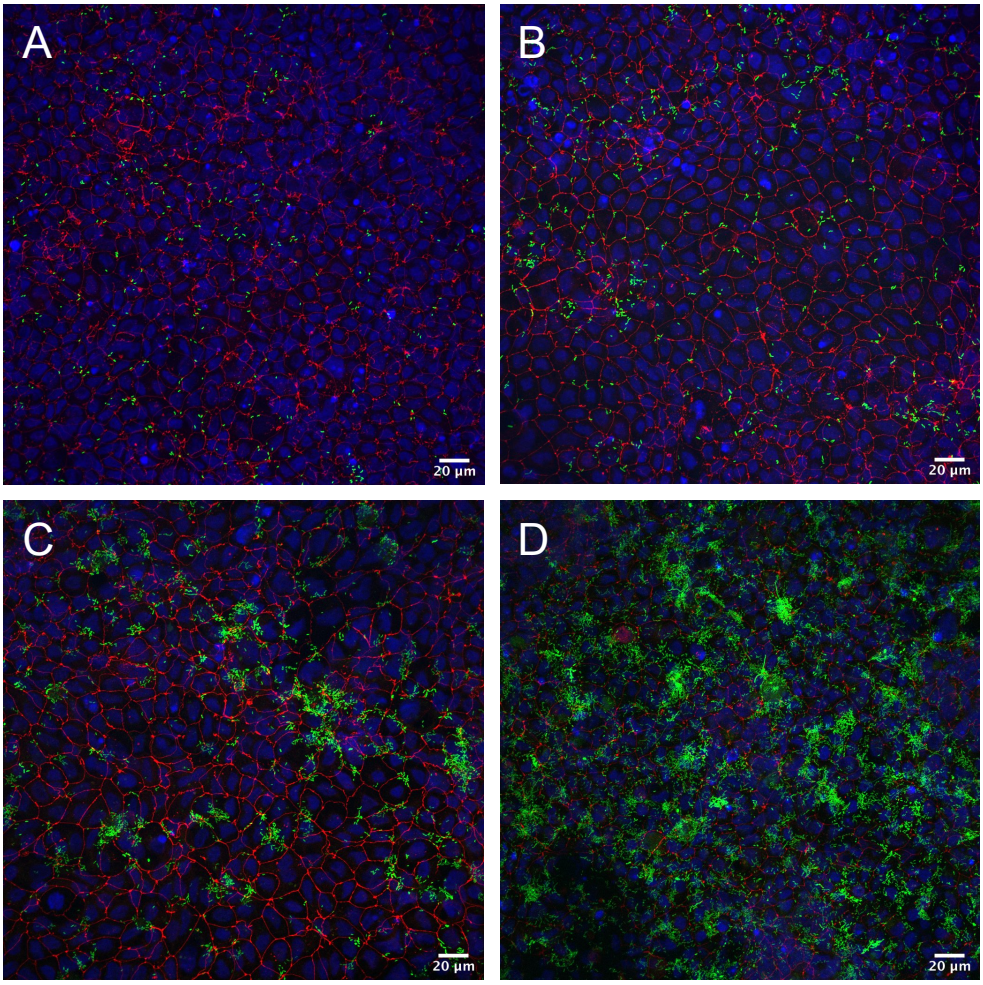

Figure 3. 4. *V. cholerae* increasingly associates with Caco-2 cell monolayers over time.

Caco-2 cell monolayers were inoculated with 5.5E5 CFU WT *V. cholerae* for incremental lengths and washed once at the end of the infection. Confocal immunofluorescence microscopy maximum intensity Z-stack projections show *V. cholerae* association with the monolayer at (A) 1, (B) 2, (C) 3, and (D) 4 hours. Red denotes tight junctions, green denotes *V. cholerae,* and dark blue denotes nuclei.

3.2. Validation of Δ*luxO V. cholerae* phenotype

LuxO is the master regulator in the *V. cholerae* quorum sensing pathway, which dictates group behaviors in a density-dependent manner [45]. At low cell density, LuxO is activated and promotes virulence factor production. At high cell density, LuxO is inactive and virulence factor production is repressed. LuxO regulates several important virulence factors, including both CTX and TCP. In a Δ*luxO* mutant, the quorum sensing pathway is always locked at the high cell density state, and production of CTX and TCP are both

repressed. Indeed, mutants lacking LuxO are severely deficient for colonization in the infant mouse model [41], [45]. Quorum sensing has also been shown to regulate GbpA, another important colonization factor, thus the Δ*luxO* mutant strain was used to validate the Caco-2 cell culture transwell system [45]–[47]. An association defect may be due to repressed production of GbpA, TCP, or other factors regulated by LuxO.

Caco-2 cell transwell monolayers were infected with WT or Δ*luxO V. cholerae* with different initial inoculums for 1.5 hours, or with 5.5E5 CFU for different time points. Bacteria associated with the monolayer were quantified by ImageJ analysis of confocal microscopy images or by CFU serial dilution plating. WT and Δ*luxO V. cholerae* quantifications by ImageJ were significantly different by unpaired t-tests with at the 2 hour- and 4 hour-post-infection time points (Figure 3.5C, D). However, quantification by direct CFU counts revealed no significant difference between WT and Δ*luxO V. cholerae* at any time point (Figure 3.5E). The difference could be explained by non-specific binding of *V. cholerae* to the walls of the transwells or areas of membranes where tight junctions had not formed properly. The differences of association between WT and Δ*luxO V. cholerae* widens over time. Confocal immunofluorescence microscopy images obtained from the 4-hour-post-infection time point show that WT *V. cholerae* associate with the Caco-2 cell monolayer more than Δ*luxO,* and they also form larger clusters resembling microcolonies (Figure 3.5F-G). These results are consistent with the previous findings obtained with animal models using the Δ*luxO* mutant strain [41], [45].

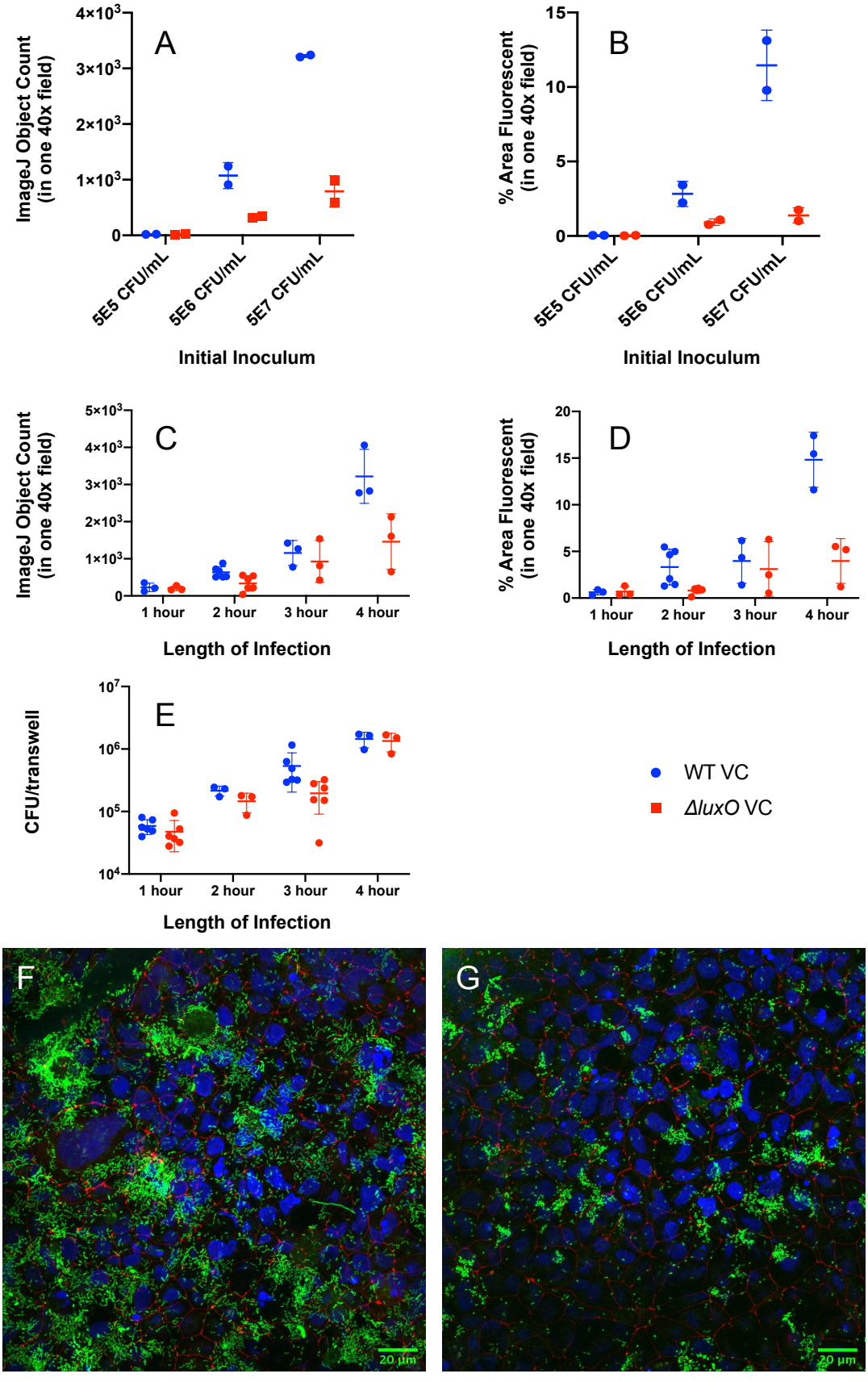
A
ImageJ Object Count (in one 40x field)
4×10^3
3×10^3
2×10^3
1×10^3
0
5E5 CFU/mL
5E6 CFU/mL
5E7 CFU/mL
Initial Inoculum
B
% Area Fluorescent (in one 40x field)
15
10
5
0
5E5 CFU/mL
5E6 CFU/mL
5E7 CFU/mL
Initial Inoculum
C
ImageJ Object Count (in one 40x field)
5×10^3
4×10^3
3×10^3
2×10^3
1×10^3
0
1 hour
2 hour
3 hour
4 hour
Length of Infection
D
% Area Fluorescent (in one 40x field)
20
15
10
5
0
1 hour
2 hour
3 hour
4 hour
Length of Infection
E
CFU/transwell
10^7
10^6
10^5
10^4
1 hour
2 hour
3 hour
4 hour
Length of Infection
WT VC
ΔluxO VC
F
20 µm
G
20 µm

Figure 3. 5. Δ*luxO V. cholerae* is deficient for association with Caco-2 cell monolayers

(A, B) Initial inoculums of 1E5, 1E6, or 1E7 CFU WT or Δ*luxO V. cholerae* were added to Caco-2 cell monolayers for 1.5 hours. Associated bacteria were observed by confocal immunofluorescence microscopy and quantified by (A) the ImageJ Object Count function or (B) the percent area fluorescent in one 40x field. Data are from one experiment with two technical replicates per inoculum per strain. By 2-way ANOVA, (A) $p<0.0001$ (****) and (B) $p=0.0011$ (**). (C, D, E) To observe association over time, 5.5E5 CFU WT or Δ*luxO V. cholerae* were added to Caco-2 cell monolayers for 1, 2, 3, or 4 hours. Associated bacteria were quantified by (C) the ImageJ Object Count function, (D) the percent area fluorescent in one 40x field, or (E) CFU plating. Individual dots are representative of (C, D) 3 technical replicates with 2 images each from 2 separate experiments and (E) 3 technical replicates per time point per strain from 2 separate experiments. By unpaired t-tests, (C, 2 hours) $p=0.0173$ (*), (C, 4 hours) $p=0.0434$ (*), (D, 2 hours) $p=0.0101$ (*), and (D, 4 hours) $p=0.0078$ (**) are significantly different. Confocal immunofluorescence microscopy maximum intensity Z-stack projections show (F) WT and (G) Δ*luxO V. cholerae* at 60x magnification 4 hours-post-infection. Red denotes tight junctions, green denotes *V. cholerae,* and dark blue denotes nuclei.

Although Δ*luxO V. cholerae* mutants are defective in attaching to the Caco-2 cells and form smaller microcolonies, the difference observed between the mutant and WT with this Caco-2 cell system is still smaller than what has been observed in the infant mouse model, where attachment is often undetectable in the host [41]. This result suggests that there are most likely several host factors involved that are not represented in this model. Moreover, there are several key differences in the Caco-2 cell culture model when compared to the infant mouse model. For example, the time points observed in this study are different from those observed in the infant mouse model (24 hours), which could contribute to the different association levels observed between the two models. Further, the bacteria do not pass through the acidic environment of the stomach in this model, which could affect gene expression. Taking a closer look at the 2-hour time point, there is a significant difference by unpaired t-test between WT and Δ*luxO V. cholerae* monolayer association early in the infection process, when small clusters of WT *V.*

cholerae are starting to form (Figure 3.6). Quantification by percent area fluorescent from confocal microscopy images most closely reflects infant mouse model colonization data between these two strains. Nevertheless, the parameters optimized with this model are useful for further testing of the enteroid model.

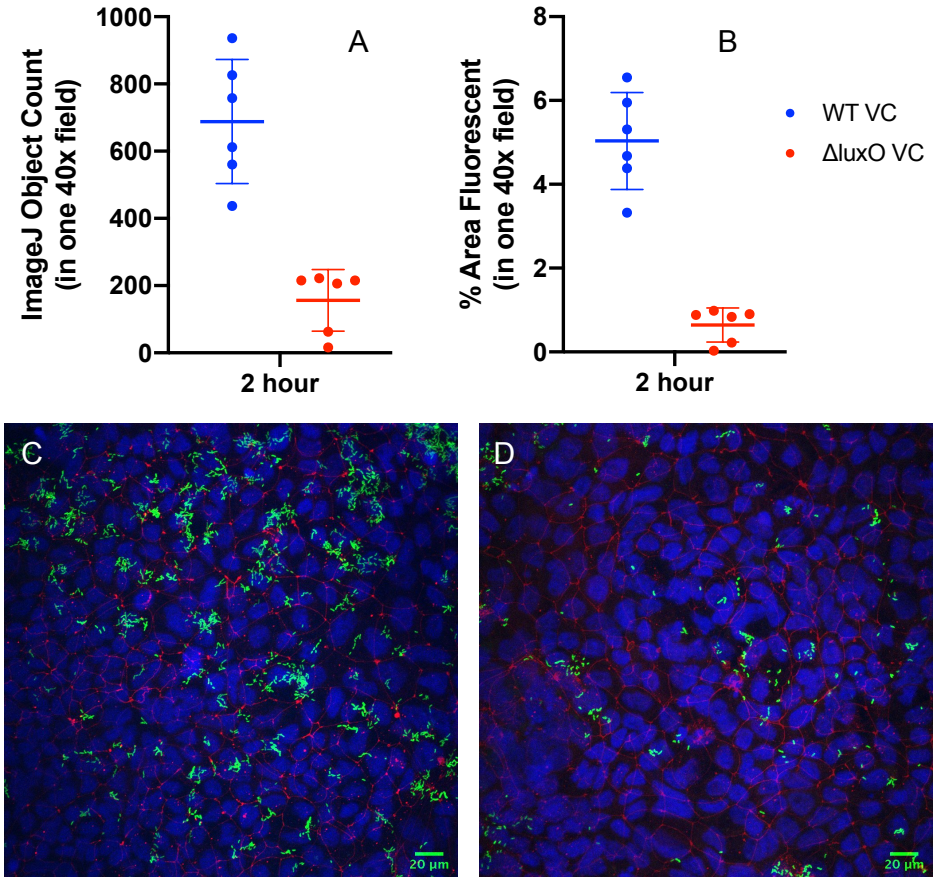

Figure 3. 6. Δ*luxO V. cholerae* is deficient for early association with Caco-2 cell monolayers

Caco-2 cell monolayers were inoculated with 5.5E5 CFU for 2 hours. Samples were washed and fixed with PFA and analyzed by confocal immunofluorescence microscopy. Associated bacteria were quantified by (A) the ImageJ Object Count function or (B) the percent area fluorescent in one 40x field. Data points are individual images, with 2 images per each of the 3 technical replicates in one experiment. By unpaired t-test, (A, B) $p<0.0001$ (****) are significantly different. Confocal immunofluorescence microscopy maximum intensity Z-stack projections show (C) WT or (D) Δ*luxO V. cholerae* association 2 hours-post-infection. Red denotes tight junctions, green denotes *V. cholerae,* and dark blue denotes nuclei.

3.3. Analysis of Caco-2 cell monolayer tight junctions

Guichard et al. 2013 showed that tight junction protein ZO-1 formed meandering paths, no longer aligned with lower adherens junctions, accumulated above nuclei, and appeared brighter after treatment with 100 ng/ml CTX every 12 hours for 36 hours [18]. Here, I tested for tight junction disruption of Caco-2 cell transwell monolayers 1 or 4 hours-post-infection with WT or Δ*luxO V. cholerae* (Figure 3.7). I hypothesized that WT would disrupt tight junctions of the monolayer and Δ*luxO V. cholerae* would not as CTX is production is repressed in the mutant. As a positive control, one transwell monolayer was treated with 200 ng/ml CTX for 24 hours. Monolayers were stained with mouse monoclonal anti-ZO-1 to observe tight junctions by confocal microscopy. Variability exists between uninfected samples. Caco-2 cell tight junctions treated for 24 hours with 200 ng/ml CTX appear brighter and some punctae were visible. However, tight junctions did not assume a meandering path and punctae were not accumulated above nuclei. In addition, there were no apparent changes to tight junctions of monolayers infected with either WT or Δ*luxO* at 1 or 4 hours, even despite abundant WT bacteria observed 4 hours-post-infection (Figure 3.7). Further optimization is required to study the effect of CTX on tight junction disruption in the 2D transwell system with *V. cholerae* bacteria.

In sum, polarized Caco-2 cell transwell monolayers were used to establish *V. cholerae* infection conditions to validate the phenotype of the well-characterized Δ*luxO* mutant in a 2D cell culture model. In some scenarios, as expected, Δ*luxO V. cholerae* was deficient in attachment to caco-2 cells when compared to WT. However, the defect was less severe than observed in the infant mouse model, and the discrepancy warrants further experimental optimization.

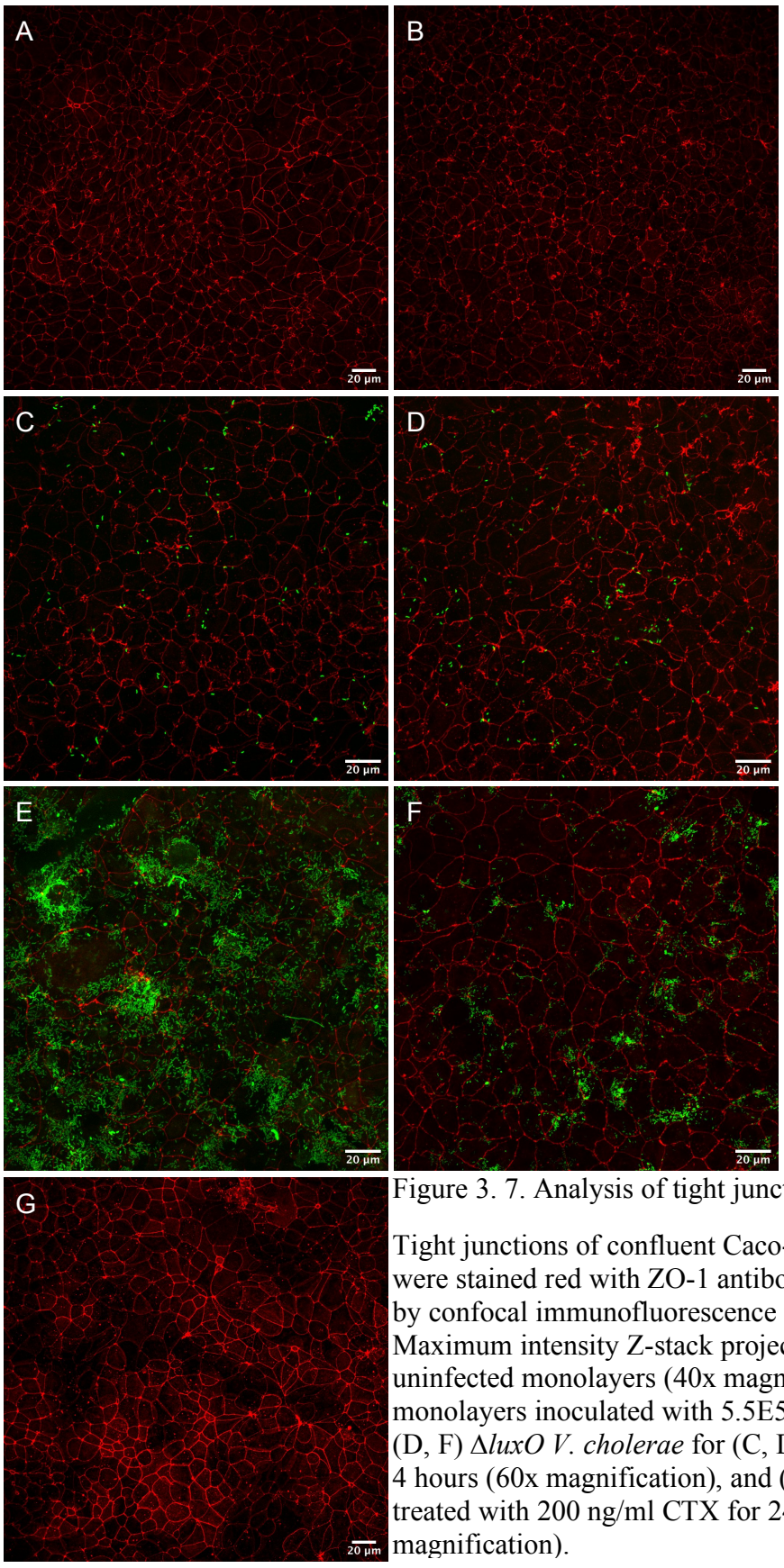

Figure 3. 7. Analysis of tight junctions

Tight junctions of confluent Caco-2 cell monolayers were stained red with ZO-1 antibody and observed by confocal immunofluorescence microscopy. Maximum intensity Z-stack projections show (A, B) uninfected monolayers (40x magnification), (C, D) monolayers inoculated with 5.5E5 CFU (C, E) WT or (D, F) Δ*luxO V. cholerae* for (C, D) 1 hour or (E, F) 4 hours (60x magnification), and (G) a monolayer treated with 200 ng/ml CTX for 24 hours (40x magnification).

Chapter 4: Establishing and Validating Enteroids as a Model for *V. cholerae* Infection

Enteroids are a promising cell culture technology for studying human-pathogen interactions. As human intestinal enteroids can be differentiated and are more physiologically relevant than other immortal cell culture systems, I hypothesized that a 2D enteroid transwell system could serve as a novel *in vitro* model to study initial attachment dynamics and early infection processes of *V. cholerae*.

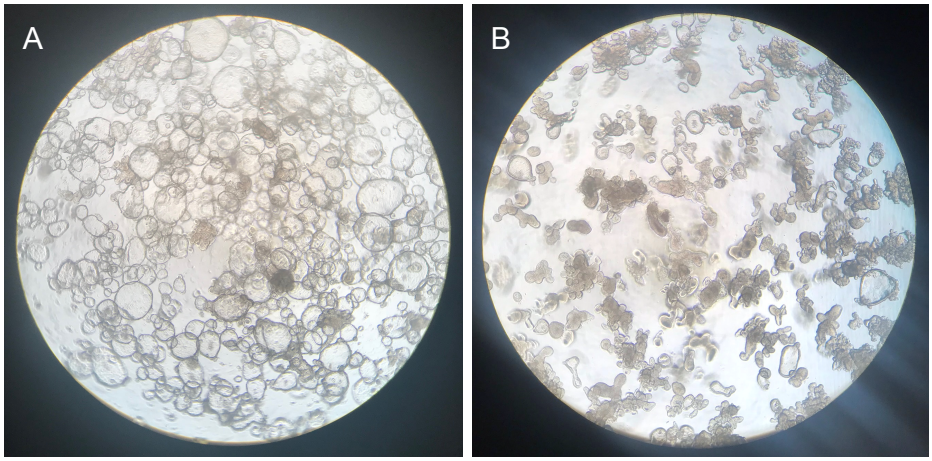

Figure 4. 1. Enteroids have two major morphologies

Undifferentiated enteroids in Matrigel grown in the presence of Wnt3a are either (A) large, clear cysts with a "soap bubble" like appearance, or (B) dark and multi-lobulated.

4.1. 3D Enteroid culture and monolayer differentiation

4.1.1. 3D Enteroids in Matrigel

Enteroid morphology is highly variable and there is no clear consensus in the literature on the correct morphology [30]–[32]. The two major morphologies I have observed are round, clear, "soap-bubble" cysts with a thin border, and multi-lobulated darker enteroids (Figure 4.1). Multi-lobulated enteroids appear to be taking on the crypt-villus structure of the small intestine, which indicates that they are beginning to differentiate.

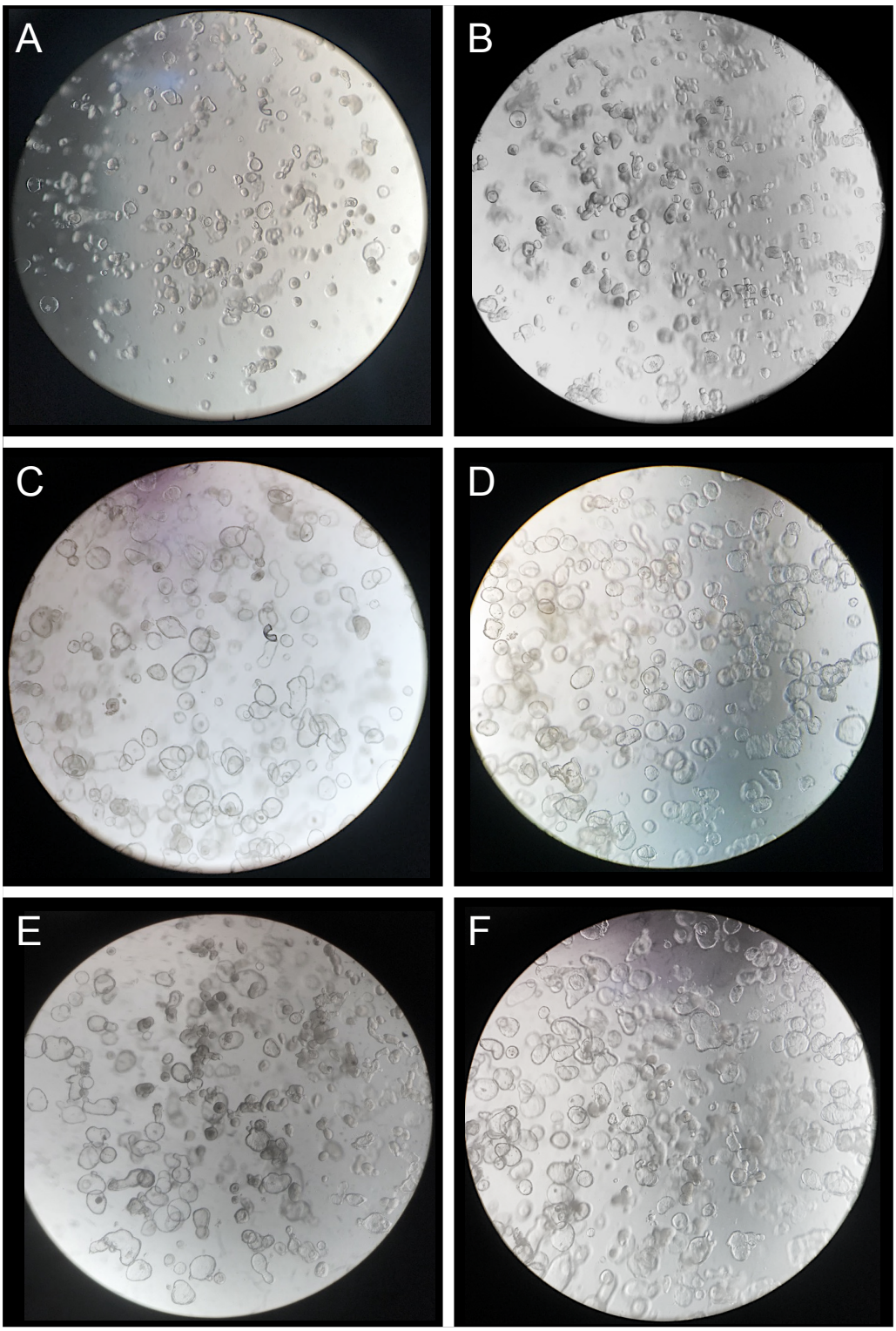

Figure 4. 2. 3D enteroids respond to CTX treatment

(A) is a representative image of pre-treated enteroids in Matrigel. Enteroids were (B) untreated or treated for 24 hours with (C) 1 µl or (D) 2 ul of PGE_2, or (E) 100 ng/ml or (F) 200 ng/ml CTX. Enteroid swelling is visible in all treated samples.

After successfully establishing the culturing of enteroids, I tested the functionality of the enteroids. CTX causes an increase in cyclic AMP levels, which in turn leads to efflux of chloride ions via the CFTR channel. Functional enteroids will swell in response to agonists including prostaglandin E_2 (PGE_2) and forskolin [29], [30], [48]. Swelling in response to PGE_2 was found to be dependent on the presence of chloride ions in the medium, and the swelling response could be blocked with CFTR channel inhibitors [48]. Thus, I hypothesize that enteroids in Matrigel treated with CTX for 24 hours would swell similarly to those treated with PGE_2. As expected, swelling response was observed in enteroids treated with either PGE_2 or CTX, but not in untreated enteroids (Figure 4.2). Further, this confirms the presence of functional CFTR channels in these enteroids, which play a key role in cholera pathology.

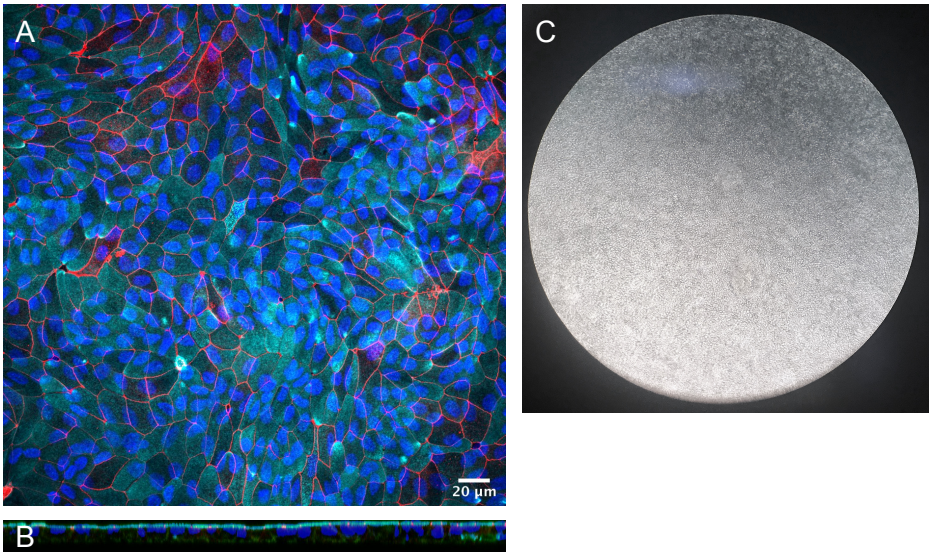

Figure 4. 3. Enteroid monolayers polarize and form tight junctions

Confocal immunofluorescence microscopy (A) Z-stack projection and (B) cross-sectional view show formation of tight junctions and polarization with a continuous apical actin brush border, representing microvilli. Red denotes tight junctions, light blue denotes actin, and dark blue denotes nuclei. (C) Single enteroid cells form a confluent monolayer, observed by light microscope.

4.1.2. Enteroids form polarized monolayers

3D enteroids can be dissociated into a single-cell state and seeded on transwells. While monolayers no longer have the cellular organization and crypt-villus architecture of the small intestine, they can still be differentiated to represent major cell types upon addition of differentiation medium. The advantages of a monolayer system are that they allow apical infection, culture in different apical and basolateral media, the presumed formation of a mucus layer, and collection of trans-epithelial experimental data. Polarized monolayers with apical microvilli and tight junctions form within 7 days and can be used for infection (Figure 4.3). 5 days-post-seeding and 3 days-post-differentiation, enterocytes, goblet cells, Paneth cells, and stem cells were quantified by qPCR (Figure 4.4). Enterocytes, the most abundant cell type, increased the most compared to undifferentiated cells 5 days-post-seeding. Mucin-2, indicating goblet cells, also

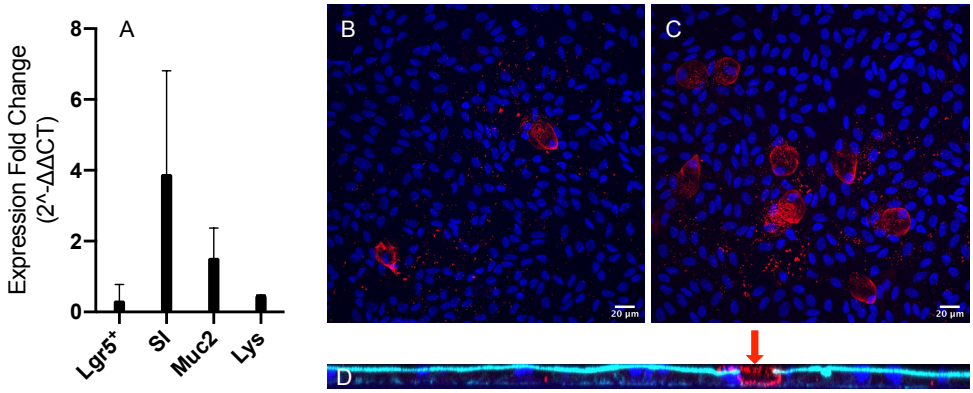

Figure 4. 4. Enteroid monolayers differentiate into 3 cell types

Enteroids grown in differentiation medium, without Wnt3a and R-Spondin, lose their stem cell state and differentiate. (A) Differentiated enteroid monolayers were harvested for qCPR 5 days-post-seeding. $Lgr5^{+}$ denotes stem cells, SI denotes enterocytes, Muc2 denotes goblet cells, and Lys denotes Paneth cells. Values are normalized to GAPDH and compared to undifferentiated enteroids 5 days-post-seeding. Values are representative of averages from 2 separate experiments, each with three technical replicates. (B) Confocal immunofluorescence microscopy maximum intensity Z-stack projections show the presence of goblet cells, denoted in red, in differentiated enteroid monolayers 7 days-post-seeding. Dark blue DAPI stain denotes nuclei.

increased as expected. Goblet cells were also confirmed by confocal immunofluorescence microscopy. The cross-sectional view shows a goblet cell, denoted in red, interrupting the continuous microvilli brush border, denoted in light blue. The number of stem cells, measured by $Lgr5^+$, decreased as expected. Paneth cells, measured by lysozyme, also decreased. This may seem unexpected, but Paneth cells are found interspersed between stem cells and play a role in their maintenance. Thus, it is logical that their presence would decline concurrently with that of stem cells. Enteroendocrine cells, the least abundant cell type, were not detected by qPCR or immunofluorescence.

In the infant rabbit model, CTX induces significant secretion of mucin from goblet cells [6]. Enteroid swelling in response to PGE_2 and CTX was quantified by qPCR. Here, enteroids treated with CTX had a marked increase in Mucin-2 levels.

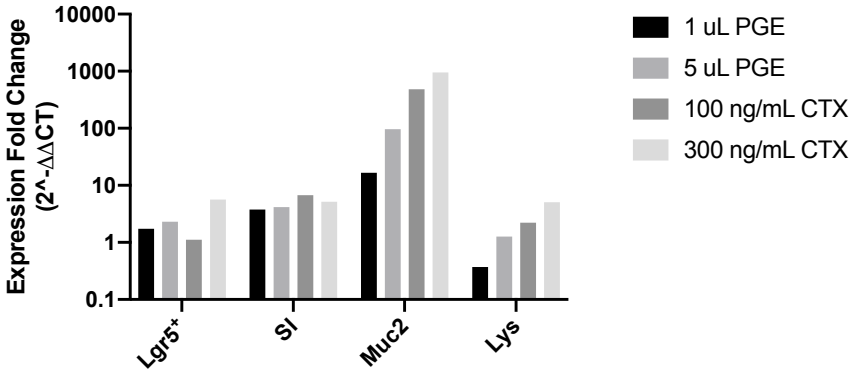

Figure 4. 5. CTX treatment induces Mucin-2 and lysozyme levels

Undifferentiated enteroids in Matrigel were treated with 1 ul PGE_2, 2 ul PGE_2, 100 ng/ml CTX, or 200 ng/ml CTX for 24 hours and harvested for qCPR. $Lgr5^+$ denotes stem cells, SI denotes enterocytes, Muc2 denotes goblet cells, and Lys denotes Paneth cells. Values are normalized to GAPDH and compared to untreated undifferentiated enteroids. Data shown represent one experiment with three technical replicates per treatment.

Further, this response was dose-dependent and was not induced to the same level by PGE_2 (Figure 4.5). CTX-treated enteroids did not have markedly higher levels of sucrase isomaltase or $Lgr5^+$ compared to PGE_2-treated enteroids. Notably, lysozyme levels

increased in a dose-dependent response to both PGE_2 and CTX treatment, but to higher levels with CTX treatment. This is perhaps a host defense response to bacterial toxin, as lysozyme is an anti-microbial agent. The molecular mechanisms underlying the increase of Mucin-2 and lysozyme production are unknown and need to be further explored.

4.2. WT *V. cholerae* associates with enteroid monolayers

One of the aims of this project is to study host-pathogen interactions with human enteroids. To test if *V. cholerae* bacteria can attach or associate with a differentiated enteroid monolayer, I first infected confluent enteroid monolayers with 1E6 CFU WT *V. cholerae* for 3 hours. Confocal immunofluorescence microscopy maximum intensity Z-stack projections show that WT *V. cholerae* associates with the enteroid monolayer (Figure 4.6). As observed in Caco-2 cell infections, *V. cholerae* associates as both individual bacteria and small clusters resembling microcolonies. Cross-sectional views of Z-stacks show clusters and individual bacteria associating with the microvilli brush border (indicated by red arrows). To study the dynamics of *V. cholerae* associated with enteroids, enteroid monolayers were infected with 1E6 CFU for 45 minutes in PBS. Infected PBS was removed after 45 minutes (denoted by a dashed red line on the graph) and replaced with fresh PBS for a specified amount of time. At each final time point, monolayers were treated with 1% Triton X-100 (confirmed non-toxic concentration to bacteria) to lyse enteroids. Samples were serially diluted and plated. CFU counts show that ~10% of the inoculum is monolayer-associated 45 minutes-post-infection. These enteroid associated *V. cholerae* bacteria replicate exponentially after 1.5 hours of infection. Bacterial cells that are unassociated were largely removed after 45 minutes, shown as red data points on the graph (Figure 4.6).

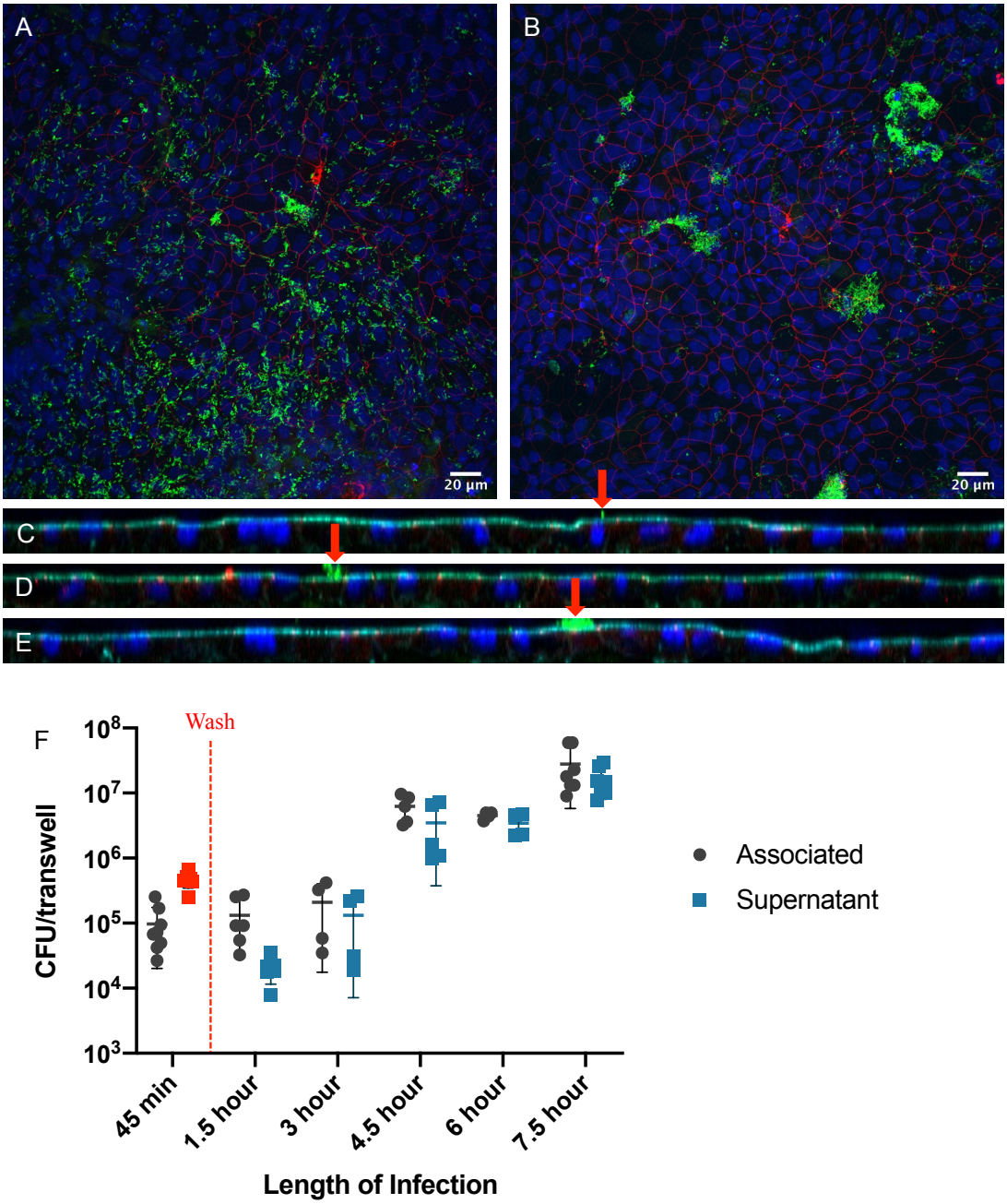

Figure 4. 6. WT *V. cholerae* associates with enteroid monolayers

Enteroid monolayers were infected with 1E6 CFU WT *V. cholerae* in PBS. (A, B) Confocal immunofluorescence microscopy maximum intensity Z-stack projections and (C-E) cross-sectional views show *V. cholerae*, in green, associated with the enteroid monolayer as individual bacteria or microcolonies 3 hours-post-infection (indicated by red arrows). (F) Infected PBS was removed at 45 minutes (red dashed line) and replaced with fresh PBS until the final time point. Samples were treated with 1% Triton X-100, serially diluted and plated for CFU. Values are from 4 separate experiments with two technical replicates per time point.

All of the bacteria both associated with the monolayer and present in the supernatant from 1.5 hours onward replicated from the ~10% of bacteria that initially associated after 45 minutes of infection. During the course of infection, about half of the bacteria are associated with the enteroid monolayer and the other half are free in the supernatant. This suggests a dynamic and heterogeneous infecting population. My results show that *V. cholerae* is capable of associating and replicating on the enteroid monolayer.

4.3. Optimization of infection media

To make the system more physiologically relevant, medium used during infection was optimized. Basolateral medium was always maintained as differentiation medium to provide nutrients to cells. Differentiation media, advanced DMEM/F12, SILAC advanced DMEM/F12 without glucose or phenol red, and PBS were tested as apical media. Differentiation media was quickly eliminated as the optimal choice because it provides nutrients to the bacteria and would repress virulence factor expression. Therefore, it was hypothesized that *V. cholerae* would associate more efficiently with the enteroid monolayer in nutrient-poor media such as PBS. To test this idea, enteroid monolayers were inoculated with 1E6 CFU *V. cholerae* for 45 minutes, then infected media was removed and replaced with respective fresh media, and infections continued for specified amounts of time (Figure 4.7). At the end of each infection, monolayers were treated with 1% Triton X-100 and samples were serially diluted and plated for CFU. By 2-way ANOVA, associated *V. cholerae* counts were significantly increased over time but there was no significant difference between the different apical media. Supernatant *V. cholerae* counts significantly increased over time and conversely, there was a significant difference for different media used. To quantify *V. cholerae* growth in fresh media (DMEM,

SILAC, and PBS) and enteroid-exposed medium (PBS that was previously exposed to an enteroid monolayer for 6 hours), 5E6 CFU/ml was inoculated into Eppendorf tubes with a different medium each for 6 hours. Number of bacteria were quantified by CFU plating. *V. cholerae* grew in DMEM, SILAC, and enteroid-exposed PBS, albeit to different extent. *V. cholerae* lost viability in PBS alone (Figure 4.7). Thus, PBS was selected as the apical medium for infections because it does not facilitate growth in the media by itself, only when factors secreted by enteroids are present, which is physiologically relevant. Interestingly, enteroid-exposed PBS allowed for ~24 fold-change in *V. cholerae* growth

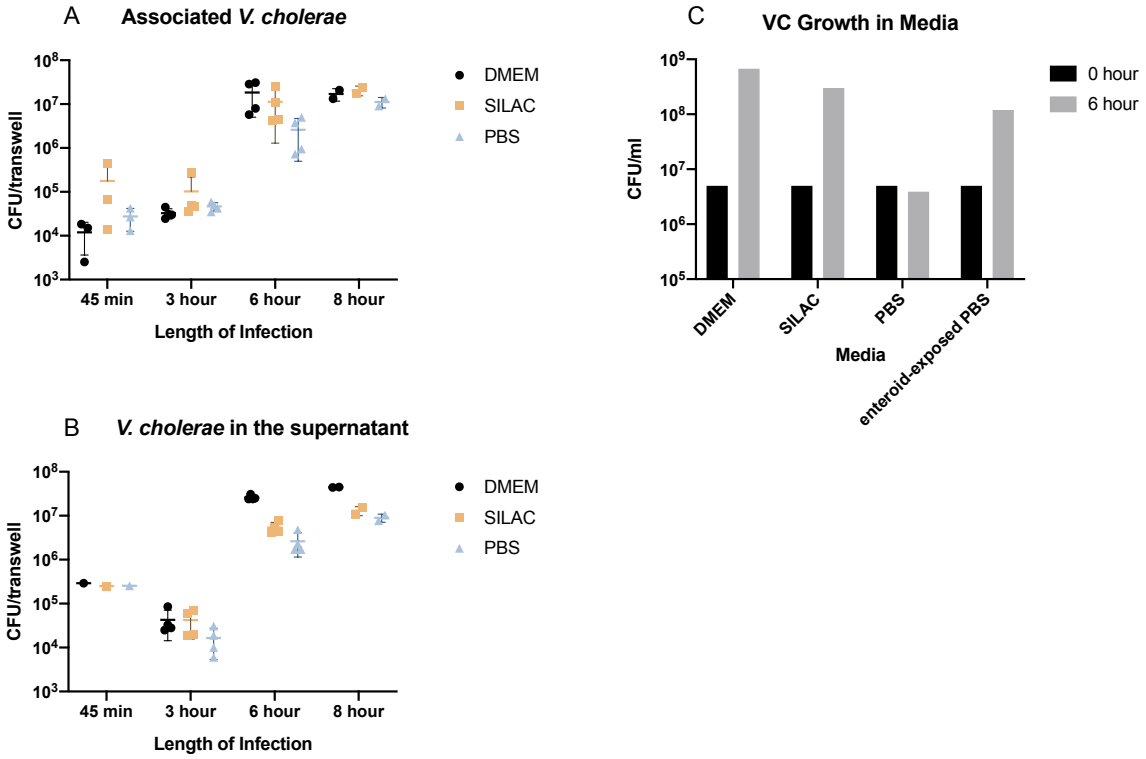

Figure 4. 7. Infection Media Comparison

Enteroid monolayers were inoculated with 1E6 CFU WT *V. cholerae* for 45 minutes, 3, 6, and 8 hours. Apical media was either DMEM, SILAC, or PBS; basolateral media was always enteroid differentiation media. *V. cholerae* grew in all 3 media in (A) association with the monolayer and (B) in the supernatant. Values are from 2 separate experiments with 2 technical replicates each. By 2-way ANOVA, (A) $p<0.0001$(****) for the row factor, time and (B) $p<0.0001$ (****) for both time and different media used. (C) Fresh media (DMEM, SILAC, and PBS) and spent media (enteroid-exposed PBS) were inoculated with 5E6 CFU/ml *V. cholerae* for 6 hours and quantified by CFU plating. Data is from one experiment.

in 6 hours, while there was ~80 fold-change in *V. cholerae* growth in 6 hours on enteroid monolayers compared to the initial amount present 45 minutes-post-infection (Figure 4.6). By 7.5 hours-post-infection of an enteroid monolayer, there is ~450 fold-change in total *V. cholerae* growth compared to the number of *V. cholerae* present 45 minutes-post-infection. This suggests that *V. cholerae* is actively extracting nutrients from the enteroid monolayer.

4.4. Validation of Δ*luxO V. cholerae* phenotype

Comparison of WT and Δ*luxO V. cholerae* association phenotypes was used to validate the enteroid transwell system. Enteroid monolayers were infected with 1E6 CFU WT or Δ*luxO V. cholerae* for 3 hours or 6 hours with one wash at the end of the infection, or incremental time points after removal of infected media and replacement with fresh media at 45 minutes. Infected monolayers were analyzed by confocal

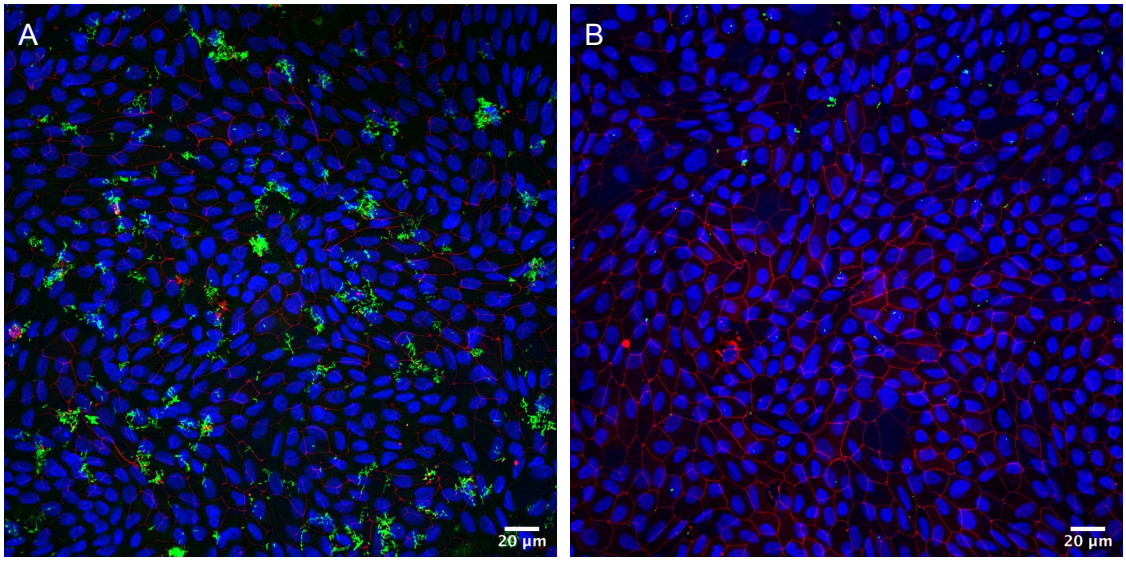

Figure 4. 8. *Δ*luxO *V. cholerae* is deficient for enteroid monolayer association

Enteroid monolayers were inoculated with 1E6 CFU for 3 hours. Samples were washed once, fixed with PFA, and analyzed by confocal immunofluorescence microscopy. Maximum intensity Z-stack projections show (A) WT or (B) Δ*luxO V. cholerae* association with the monolayer. Red denotes tight junctions, green denotes *V. cholerae,* and dark blue denotes nuclei.

immunofluorescence microscopy (Figure 4.8) or CFU plating (Figure 4.9). All data were analyzed by unpaired t-tests. At 3 hours, there are significantly more WT associated than Δ*luxO* for quantification by percent area fluorescent, but not for object count. For 3-hour graphs, individual dots represent the average of 3 to 4 technical replicates, each with 1 to 2 images each, from 5 (4.9A) or 4 (4.9B) different experiments. At 6 hours, there are significantly more WT associated than Δ*luxO* when quantified by object count, but not by percent area fluorescent. WT demonstrates variability in association with the monolayer while Δ*luxO* consistently associates at low levels. For 6-hour graphs, individual dots are 4 technical replicates per strain from one experiment. There are significantly more WT *V. cholerae* than Δ*luxO* associated 6 hours-post-infection when quantified by object count. In figure 4.9E, F, WT *V. cholerae* association is significantly different at all time points, with an increase in difference over time. Interestingly, there was no significant difference between Δ*luxO* association at 3, 4 and 5 hours. This is different than what was observed in the Caco-2 cell monolayer infection, where Δ*luxO* numbers did increase over time (Figure 3.5). However, double layers were observed in cross-sectional views of images analyzed in figure 4.9E, F, and thus this experiment needs to be repeated with monolayers and the presence of double layers should be considered when concluding from this data. Further, enteroid monolayer tight junctions were not damaged 3 hours-post-infection with 1E6 CFU WT or Δ*luxO V. cholerae*. Tight junctions appeared normal by confocal immunofluorescence microscopy and tight junction integrity was not compromised 6 hours-post-infection as determined by the HRP assay (data not shown).

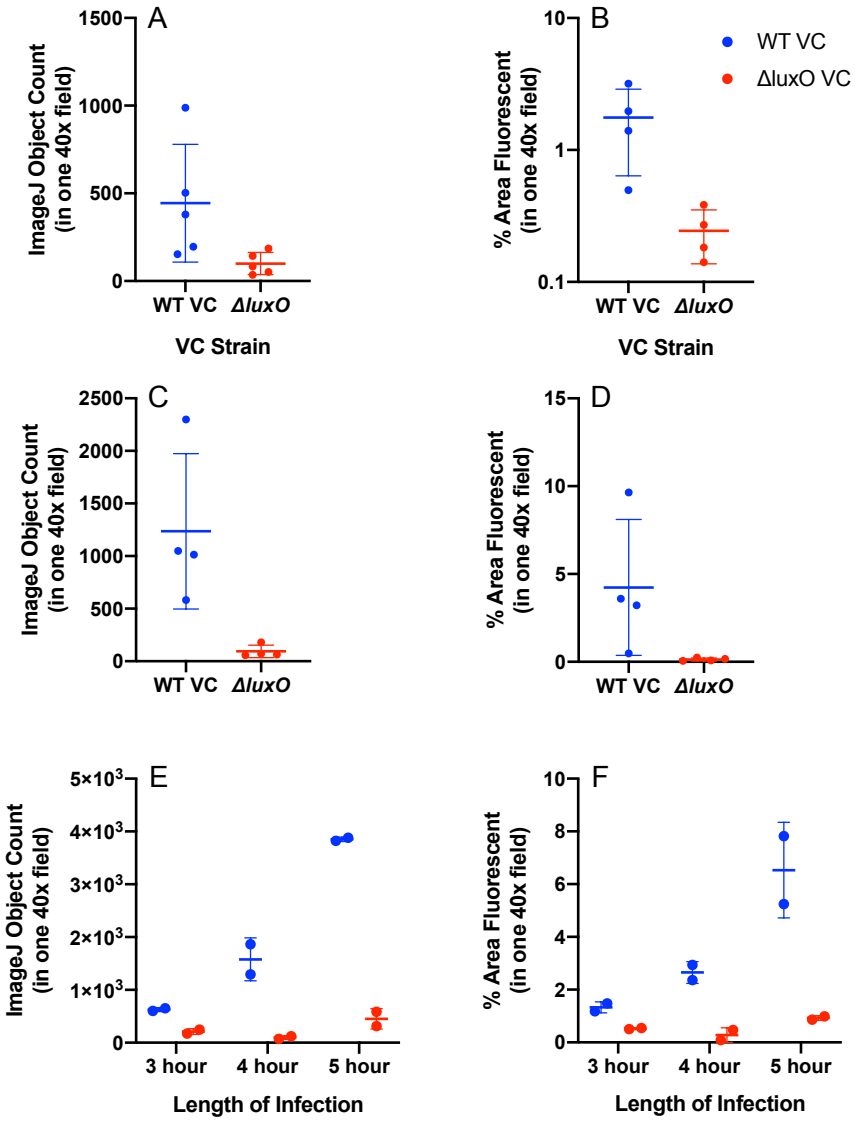

Figure 4. 9. ΔluxO *V. cholerae* association deficiency increases over time

Enteroid monolayers were inoculated with 1E6 CFU for (A, B) 3 hours without wash until the end, (C, D) 6 hours without wash until the end, or (E, F) incremental time points, all washed once at 1.5 hours-post-infection. Associated bugs were quantified by (A, C, E) the ImageJ Object Count function or (B, D, F) the percent area fluorescent in one 40x field. Individual dots are representative of averages from (A) 5 or (B) 4 separate experiments with 3 to 4 technical replicates per strain with 1 to 2 images per technical replicate each. By unpaired t-test, (B) p=0.0362 (*) is significantly different. (C, D) Values are from 4 technical replicates per strain from one experiment. By unpaired t-test, (C) p=0.0217 (*) is significantly different. (E, F) Dots are values from 2 technical replicates per strain per time point from one experiment. By unpaired t-tests, (E, 3 hour) p=0.0123 (*), (E, 4 hour) p=0.0358 (*), (E, 5 hour) p=0.0017 (**), (F, 3 hour) p=0.0325 (*), (F, 4 hour) p=0.0209 (*), (F, 5 hour) p=0.0488 (*) are significant different.

4.5. Simulating intestinal flow with washes

V. cholerae in the small intestine are exposed to mechanical forces like flow and peristalsis. These factors are not yet incorporated into the enteroid transwell model. To simulate flow, washes (removal of infected medium and replacement with fresh medium) were performed throughout the course of the infection. Enteroid monolayers were infected with 1E6 CFU WT or Δ*luxO V. cholerae* for 3 hours and were washed once at the end, twice at 1.5 hours and the end, or thrice at 1 hour, 2 hours and the end of the infection (Figure 4.10). Infected monolayers were analyzed by confocal immunofluorescence microscopy. Washing at 1.5 hours minimized variability, and fewer

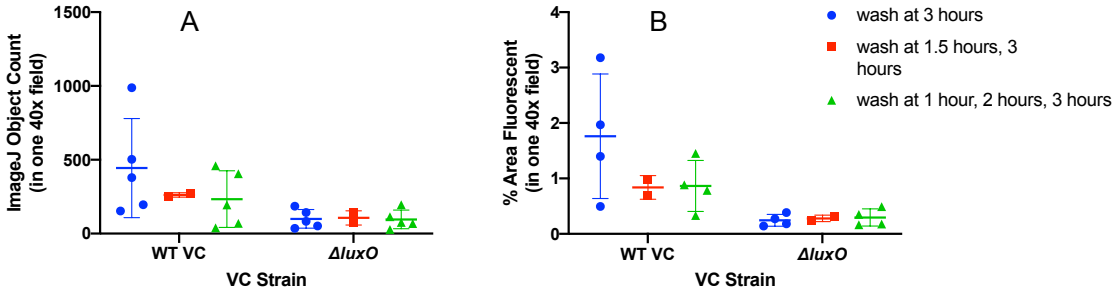

Figure 4. 10. Washing decreases WT association but does not affect Δ*luxO V. cholerae* association

Enteroid monolayers were inoculated with 1E6 CFU for 3 hours. Infected media was removed and replaced with fresh media as indicated by washes (blue denotes one wash at 3 hours, red denotes two washes (1.5 hours and 3 hours), and green denotes three washes (1 hour, 2 hours, and 3 hours)). Samples were analyzed by confocal immunofluorescence microscopy and quantified by (A) ImageJ Object Count function or (B) the percent area fluorescent. Individual dots are representative of averages from 5 (blue dots and green triangles) or 2 (red squares) separate experiments with 3 to 4 technical replicates per strain with 1 to 2 images per technical replicate. By 2-way ANOVA, (A) p=0.0056 (**) for the row factor, *V. cholerae* strain, and (B) p=0.0208 (*) for the row factor, *V. cholerae* strain. There is no significant difference for the column factor, washes, for either strain in A or B.

WT *V. cholerae* associated with the monolayer with more washes. Δ*luxO* was not affected by washes, perhaps suggesting that any association observed for this mutant strain is non-specific and at a basal level even without washing. WT *V. cholerae* may

have a heterogeneous infecting population and thus only those bacteria producing a certain virulence factor are able to withstand washing and remain associated.

As observed in Caco-2 cell monolayers, WT *V. cholerae* associate more with an enteroid monolayer than Δ*luxO V. cholerae*. Conversely, Δ*luxO V. cholerae* association did not increase over time as seen in Caco-2 cell monolayers. Importantly, Figure 4.6 and 4.7 suggest that WT *V. cholerae* is actively obtaining nutrients from the enteroid monolayer, as growth in the presence of a monolayer is higher than growth in enteroid-exposed PBS with no monolayer. Damage to tight junctions was not detected here, but CTX treatment caused 3D enteroid swelling and induced Mucin-2 and lysozyme levels. These preliminary optimization and validation studies suggest that both 2D and 3D enteroids are still a promising system to study *V. cholerae in vitro.*

Chapter 5: Discussion.

In this study, enteroids were evaluated as a novel model system for studying *V. cholerae.* To do this, a Caco-2 cell transwell monolayer system was used to optimize protocols and validate the well-characterized Δ*luxO* mutant, which had not previously been validated in any cell culture model. In Caco-2 cells, an association deficiency was observed by confocal immunofluorescence microscopy analysis, but not by CFU plating, for Δ*luxO* compared to WT *V. cholerae.* However, decreased Δ*luxO V. cholerae* association was much less pronounced than in the infant mouse model. While the infant mouse model has limitations, it is a more complex system in ways because it includes factors like intestinal flow, peristalsis, and competition from other microbiota. The smaller difference observed in the Caco-2 cell model may indicate that in the absence of one of these factors, LuxO and the genes it regulates are not important for epithelial association. In the enteroid monolayer system, a larger association deficiency between WT and Δ*luxO V. cholerae* was observed, closer to that in the infant mouse model. Though, it should be noted that the apical media used during infection of Caco-2 cells (DMEM) and enteroids (PBS) was different. Yet, the data in figure 4.7A show that the number of bacteria associated with enteroid monolayers is not significantly different in DMEM or PBS. Thus, enteroid monolayers may be more similar to the actual intestinal environment of the host including different cell types and mucin production.

About 10% of WT *V. cholerae* associate with the enteroid monolayer 45 minutes-post-infection. From this associated population, replication occurred over time and some bacteria remained associated and some swam into the supernatant. There was a ~450 fold-change in *V. cholerae* numbers from the initially associated population at 45 minutes

to 7.5 hours-post-infection, or about 7 hours from the 45-minute time point. This growth was surprisingly large compared to *V. cholerae* growth in enteroid-exposed PBS, which led to ~24 fold-change. Some nutrients in the apical media (either the supernatant during infection or the enteroid-exposed PBS) may be due to diffusion of nutrients from the basolateral media (differentiation media) and enteroid-secreted nutrients. However, the large difference in fold-change based on the presence of a live enteroid monolayer suggests that *V. cholerae* is actively extracting nutrients from the enteroid monolayer. Recently, Rivera-Chavez et al. used an infant rabbit model to show that *V. cholerae* acquires nutrients including haem and long-chain fatty acids from the host, and that this function is dependent on CTX [49]. It would be interesting to investigate this in the enteroid transwell model. To start, the growth of a Δ*ctx* mutant strain can be compared to growth of WT *V. cholerae* on enteroid monolayers. If the Δ*ctx* mutant strain is deficient for growth, it would suggest that *V. cholerae* is growing exponentially due to nutrients extracted from the host in a CTX-dependent manner.

When monolayers were washed throughout the infection, WT *V. cholerae* association decreased with more washing and Δ*luxO V. cholerae* association was not affected. It is possible that Δ*luxO* association is not affected because any association observed with or without washing is non-specific or a basal amount of association. A function of intestinal flow is to flush the GI tract of unwanted material, including pathogenic bacteria. Washing may simulate this aspect, making it more difficult for bacteria to associate. However, the effects from the force of washing with a pipette are likely different from those of washing by continual, gentler flow in the intestine. Tangentially, it should be determined if the force of washing too easily removes

associated bacteria. To test this, infected media can be removed, replaced with fresh media for a few minutes, and then removed to quantify the number of bacteria present in the second wash. If there are many bacteria present in the second wash after only a short exposure to the monolayer, this would suggest that the force of washing was removing the bacteria, and not that the bacteria were dissociating naturally and swimming into the supernatant. Variability observed in WT *V. cholerae* association with washes could indicate heterogeneity in the infecting population where only bacteria expressing a certain factor are able to withstand washing. Washing also removes accumulated autoinducer signaling molecules that activate the quorum sensing pathway. WT *V. cholerae* would be susceptible to changes in levels of autoinducers. With fewer autoinducers, bacteria would assume a low cell density state and express virulence factors. It may be expected that WT *V. cholerae* would increasingly associate with more washes, but that was not observed in this model. Perhaps WT *V. cholerae* association is influenced more strongly by the mechanical force of washing than levels of autoinducers in this model. An alternate explanation could be that the increased expression of virulence factors like TCP is not important in this model. It has been suggested that TCP may play a role later in colonization and not in direct attachment to the monolayer. It was previously reported that TCP was deficient for colonization of a Caco-2 cell monolayer 3 hours-post-infection, but the mutant strain defect was not complemented by a plasmid over-expressing TCP [10]. Thus, the role of TCP has not been solidly established in cell culture models and may not play a role in early infection or in static, simpler systems that lack components like an acid stomach environment, intestinal flow and peristalsis. Mannose-sensitive hemagglutinin (MSHA) has been proposed as the main attachment

factor for El Tor *V. cholerae* strains and TCP as the major factor for classical strain [50, pp. 278–280], [51]. Here, an El Tor *V. cholerae* strain was used for experiments. It remains unclear if TCP is an important factor for El Tor *V. cholerae* association in this model.

Quantification with ImageJ analysis of confocal immunofluorescence microscopy Z-stacks is a better method than CFU plating for this system. Without visualizing the bacteria quantified as when quantifying by CFU plating, bacteria that are stuck in small gaps in the monolayer or on the sides of the transwells may also be quantified, leading to an apparently smaller difference in association between the WT and Δ*luxO V. cholerae*. Confocal immunofluorescence microscopy gives information about bacterial association as single bacteria, small clusters, or microcolonies. Clusters and early microcolonies were apparent in WT-infected monolayers and less so in Δ*luxO*-infected monolayers. It would be expected that Δ*luxO* does not associate as clusters or microcolonies, because *tcpA* is repressed, and TcpA is known to play a role in microcolony formation. This difference was again more apparent in enteroid monolayers than in Caco-2 cell monolayers. ImageJ object count function and percent area fluorescent calculations complement each other and together account for variability when analyzing single bacteria or clusters. Object count is useful when bacteria are dispersed and associated as single bacteria; percent area fluorescent measurements may introduce error in quantifying single bacteria that are perpendicular or parallel to the monolayer. Percent area fluorescent is much more accurate when quantifying images with clusters of bacteria, as the object count function will only count a cluster as one object, when in reality, a cluster is many bacteria. An additional method of quantification could be to determine various sizes of clusters or

microcolonies in the image, and to present this data as a scatterplot of the different size groups. This would give information about how many bacteria associated as single bacteria, small clusters, or large clusters/microcolonies.

The effects of cholera toxin on 2D enteroid monolayer tight junctions were observed by confocal immunofluorescence microscopy and the HRP assay. Contrary to what has previously been reported, tight junctions visibly remained unchanged when infected with WT *V. cholerae* or *luxO V. cholerae* for 3 hours. The HRP assay suggests that there was no loss of tight junction integrity and that they remained intact. However, HRP is about 44 kd, which is rather large and may not detect early damage or damage that would allow very tiny molecules of relevance, like sodium ions and water molecules, to cross the barrier. A FITC-dextran assay, as previously used in the rabbit ligated ileal loop model, may be more accurate for determining barrier integrity [19]. Another potential method to measure tight junction integrity could be with biotinylation of the apical surface and quantifying biotin that traversed to the basolateral side post-infection. The difference in results observed here compared to results previously observed by Guichard et al. could be explained by differences in experiment setup. Here, early time points of 3 to 6 hours were assessed, while Guichard et al. reported effects after 36 hours [18]. Importantly, a key difference is treatment with purified CTX or whole *V. cholerae* bacteria. It is possible that by 3 to 6 hours of infection, *V. cholerae* does not produce enough CTX to cause damage. The effects of CTX were better observed in the 3D enteroid model. A 24-hour treatment of 3D enteroids with purified CTX led to a swelling response and Mucin-2 and lysozyme induction. A mucus barrier and lysozyme anti-microbial molecules are innate immunity components that cells use as defense against

pathogens. It has been previously suggested that goblet cells are depleted of Mucin-2 storage when treated with CTX [6]. Further, it has been shown that *V. cholerae* preferentially colonize the crypts, where Paneth cells that produce lysozyme reside.

After this initial validation, both 2D and 3D enteroid systems remain promising as novel models for studying *V. cholerae.* 2D enteroid monolayers may be the preferred cell culture model for studies looking at earlier time points of infection. Results in this system were similar to what was previously observed in an infant mouse model. In addition, studying damage caused by *V. cholerae* to human epithelial cells is more relevant with human ileal enteroids than colon adenocarcinoma-derived Caco-2 cells. Results from this study suggest that 3D enteroids will be useful for investigating damage and host cell response to CTX treatment.

However, these systems should continue to be optimized to add more relevance. Importantly, it is often stated that enteroid monolayers have a mucus layer. While Mucin-2 levels increase by qPCR and goblet cells can be detected by confocal immunofluorescence microscopy, this does not guarantee a mucus layer in the 2D enteroid monolayer system at the time of infection. Removal of media and washing may or may not disturb or abolish the mucus layer. Additionally, N-acetylcysteine, a component of enteroid $CMGF^+$ medium, is a known mucolytic agent that disrupts disulfide bonds between mucins [9]. It is sometimes used in experiments to remove the mucus layer. Therefore, it needs to be determined if the concentration of N-acetylcysteine in the medium is disrupting the mucus layer. To do this, the mucus layer could be visualized with a probe such as wheat germ agglutinin or periodic acid-Schiff/Alcian Blue stain. Recently developed protocols for apical-out enteroids may be useful for

studying *V. cholerae* infection in the 3D enteroid state. The advantages of this include *V. cholerae* having access to the apical surface as in a typical infection and maintenance of crypt-villus architecture with signaling gradients, which is a key functional component of the small intestine. 3D enteroids also present an opportunity to study potential drugs that would block the effects of CTX and simultaneously monitor the side effects of these drugs on human epithelial cells. This would be an important advantage as many human drug trials fail due to unexpected toxicity or inefficacy in humans.

In 2D enteroid monolayer infections, *V. cholerae* were observed associated with the monolayer and free in the supernatant by CFU plating analysis. Using this model, it would be interesting to investigate differences in gene expression between the monolayer-associated and free-swimming bacteria and determine if there are two distinct populations that exist. It has been previously suggested that there is heterogeneity in the infecting population and that early attachment is a dynamic process [7], [8], [13]. Several observed results support this notion of heterogeneity. Bacteria are observed both associated with the monolayer and free in the supernatant. They attach as single bacteria and clusters resembling microcolonies. Third, there is variability in the numbers of WT *V. cholerae* that associate between technical and biological replicates. The functional importance of this apparent heterogeneity is an unanswered question [6], [13].

The 2D enteroid monolayer model is conducive to studying earlier time points of infection. To continue investigating factors involved in initial association or attachment, mutant strains can be compared to WT *V. cholerae*, similar to the studies completed here with Δ*luxO.* Genes that have been suggested to play a role in initial association in other models include *gbpA*, *mam7*, and *ompU.* As mentioned above, it would also be important

to investigate a Δ*mshA* mutant strain. While preliminary results, quantified by CFU plating, from the 2D enteroid monolayer system suggest that Δ*tcpA* is not deficient for association compared to WT *V. cholerae* (data not shown), it may be interesting to investigate this comparison by confocal immunofluorescence microscopy, which is a more sensitive quantification method. Additionally, it would be interesting to observe if a Δ*tcpA* mutant formed clusters or microcolonies as observed in WT infections. It would be hypothesized that they would associate primarily as single bacteria.

In sum, human ileal enteroids have been preliminarily validated as an alternative model for studying *V. cholerae* pathogenesis. The 2D enteroid transwell monolayer system can be used to investigate the factors that are important for initial association and attachment. It can also be used to study the dynamics and heterogeneity of the initial infection process. The 3D enteroid model will serve as a useful tool for studying damage caused to human small intestinal cells and the host cell response and defense mechanisms.

Chapter 6: Bibliography

[1] J. R. Thiagarajah and A. S. Verkman, "New drug targets for cholera therapy," *Trends Pharmacol. Sci.*, vol. 26, no. 4, pp. 172–175, Apr. 2005.

[2] K. Bharati and N. K. Ganguly, "Cholera toxin: a paradigm of a multifunctional protein," *Indian J. Med. Res.*, vol. 133, no. 2, pp. 179–187, Feb. 2011.

[3] World Health Organization, "Weekly epidemiological record," World Health Organization, No 38, 2018, 93, Sep. 2018.

[4] L. Shen, "Functional Morphology of the Gastrointestinal Tract," in *Molecular Mechanisms of Bacterial Infection via the Gut*, vol. 337, C. Sasakawa, Ed. Berlin, Heidelberg: Springer Berlin Heidelberg, 2009, pp. 1–35.

[5] F. E. Holmberg *et al.*, "Culturing human intestinal stem cells for regenerative applications in the treatment of inflammatory bowel disease," *EMBO Mol. Med.*, vol. 9, no. 5, p. 558, May 2017.

[6] J. M. Ritchie, H. Rui, R. T. Bronson, and M. K. Waldor, "Back to the future: studying cholera pathogenesis using infant rabbits," *mBio*, vol. 1, no. 1, pp. e00047-10, May 2010.

[7] S. Almagro-Moreno, K. Pruss, and R. K. Taylor, "Intestinal Colonization Dynamics of Vibrio cholerae," *PLOS Pathog.*, vol. 11, no. 5, p. e1004787, May 2015.

[8] A. M. Spagnuolo, V. Dirita, and D. Kirschner, "A model for Vibrio cholerae colonization of the human intestine," *J. Theor. Biol.*, vol. 289, pp. 247–258, Nov. 2011.

[9] Y. A. Millet, D. Alvarez, S. Ringgaard, U. H. von Andrian, B. M. Davis, and M. K. Waldor, "Insights into Vibrio cholerae Intestinal Colonization from Monitoring Fluorescently Labeled Bacteria," *PLOS Pathog.*, vol. 10, no. 10, p. e1004405, Oct. 2014.

[10] S. J. Krebs and R. K. Taylor, "Protection and attachment of Vibrio cholerae mediated by the toxin-coregulated pilus in the infant mouse model," *J. Bacteriol.*, vol. 193, no. 19, pp. 5260–5270, Oct. 2011.

[11] K. H. Thelin and R. K. Taylor, "Toxin-coregulated pilus, but not mannose-sensitive hemagglutinin, is required for colonization by Vibrio cholerae O1 El Tor biotype and O139 strains.," *Infect. Immun.*, vol. 64, no. 7, pp. 2853–2856, Jul. 1996.

[12] D. A. Herrington, R. H. Hall, G. Losonsky, J. J. Mekalanos, R. K. Taylor, and M. M. Levine, "Toxin, toxin-coregulated pili, and the toxR regulon are essential for Vibrio cholerae pathogenesis in humans," *J. Exp. Med.*, vol. 168, no. 4, pp. 1487–1492, Oct. 1988.

[13] J. M. Ritchie and M. K. Waldor, "Vibrio cholerae Interactions with the Gastrointestinal Tract: Lessons from Animal Studies," in *Molecular Mechanisms of Bacterial Infection via the Gut*, vol. 337, C. Sasakawa, Ed. Berlin, Heidelberg: Springer Berlin Heidelberg, 2009, pp. 37–59.

[14] T. J. Kirn, M. J. Lafferty, C. M. P. Sandoe, and R. K. Taylor, "Delineation of pilin domains required for bacterial association into microcolonies and intestinal colonization by Vibrio cholerae," *Mol. Microbiol.*, vol. 35, no. 4, pp. 896–910, Feb. 2000.

[15] V. Sperandio, J. A. Girón, W. D. Silveira, and J. B. Kaper, “The OmpU outer membrane protein, a potential adherence factor of Vibrio cholerae,” *Infect. Immun.*, vol. 63, no. 11, pp. 4433–4438, Nov. 1995.
[16] A. M. Krachler, H. Ham, and K. Orth, “Outer membrane adhesion factor multivalent adhesion molecule 7 initiates host cell binding during infection by Gram-negative pathogens,” *Proc. Natl. Acad. Sci.*, vol. 108, no. 28, p. 11614, Jul. 2011.
[17] T. J. Kirn, B. A. Jude, and R. K. Taylor, “A colonization factor links Vibrio cholerae environmental survival and human infection,” *Nature*, vol. 438, no. 7069, pp. 863–866, Dec. 2005.
[18] A. Guichard *et al.*, “Cholera Toxin Disrupts Barrier Function by Inhibiting Exocyst-Mediated Trafficking of Host Proteins to Intestinal Cell Junctions,” *Cell Host Microbe*, vol. 14, no. 3, pp. 294–305, Sep. 2013.
[19] S. Sawasvirojwong, P. Srimanote, V. Chatsudthipong, and C. Muanprasat, “An Adult Mouse Model of Vibrio cholerae-induced Diarrhea for Studying Pathogenesis and Potential Therapy of Cholera,” *PLoS Negl. Trop. Dis.*, vol. 7, no. 6, p. e2293, Jun. 2013.
[20] S. H. Richardson, “Animal Models in Cholera Research,” in *Vibrio cholerae and Cholera*, I. K. Wachsmuth, Ø. Olsvik, and P. A. Blake, Eds. American Society of Microbiology, 1994, pp. 203–226.
[21] K. E. Klose, “The suckling mouse model of cholera,” *Trends Microbiol.*, vol. 8, no. 4, pp. 189–191, Apr. 2000.
[22] S. Abel and M. K. Waldor, “Infant Rabbit Model for Diarrheal Diseases,” *Curr. Protoc. Microbiol.*, vol. 38, p. 6A.6.1-6A.6.15, Aug. 2015.
[23] P. Panigrahi, B. D. Tall, R. G. Russell, L. J. Detolla, and J. G. Morris Jr, “Development of an in vitro model for study of non-O1 Vibrio cholerae virulence using Caco-2 cells,” *Infect. Immun.*, vol. 58, no. 10, pp. 3415–3424, Oct. 1990.
[24] R. K. Yu, S. Usuki, Y. Itokazu, and H.-C. Wu, “Novel GM1 ganglioside-like peptide mimics prevent the association of cholera toxin to human intestinal epithelial cells in vitro,” *Glycobiology*, vol. 26, no. 1, pp. 63–73, Jan. 2016.
[25] D. L. Bourque *et al.*, “Analysis of the Human Mucosal Response to Cholera Reveals Sustained Activation of Innate Immune Signaling Pathways,” *Infect. Immun.*, vol. 86, no. 2, pp. e00594-17, Jan. 2018.
[26] R. Balamurugan, A. S. Chandragunasekaran, G. Chellappan, K. Rajaram, G. Ramamoorthi, and B. S. Ramakrishna, “Probiotic potential of lactic acid bacteria present in home made curd in southern India,” *Indian J. Med. Res.*, vol. 140, no. 3, pp. 345–355, Sep. 2014.
[27] K. Kozuka *et al.*, “Development and Characterization of a Human and Mouse Intestinal Epithelial Cell Monolayer Platform,” *Stem Cell Rep.*, vol. 9, no. 6, pp. 1976–1990, Dec. 2017.
[28] T. Sato *et al.*, “Long-term Expansion of Epithelial Organoids From Human Colon, Adenoma, Adenocarcinoma, and Barrett’s Epithelium,” *Gastroenterology*, vol. 141, no. 5, pp. 1762–1772, Nov. 2011.
[29] J. Foulke-Abel *et al.*, “Human enteroids as an *ex-vivo* model of host–pathogen interactions in the gastrointestinal tract,” *Exp. Biol. Med.*, vol. 239, no. 9, pp. 1124–1134, Sep. 2014.

[30] K. Saxena *et al.*, "Human Intestinal Enteroids: a New Model To Study Human Rotavirus Infection, Host Restriction, and Pathophysiology," *J. Virol.*, vol. 90, no. 1, pp. 43–56, Jan. 2016.
[31] G. Noel *et al.*, "A primary human macrophage-enteroid co-culture model to investigate mucosal gut physiology and host-pathogen interactions," *Sci. Rep.*, vol. 7, p. 45270, Mar. 2017.
[32] W. Y. Zou *et al.*, "Human Intestinal Enteroids: New Models to Study Gastrointestinal Virus Infections," Totowa, NJ: Humana Press, 2017.
[33] J. Y. Co *et al.*, "Controlling Epithelial Polarity: A Human Enteroid Model for Host-Pathogen Interactions," *Cell Rep.*, vol. 26, no. 9, p. 2509–2520.e4, Feb. 2019.
[34] A. Fatehullah, S. H. Tan, and N. Barker, "Organoids as an in vitro model of human development and disease," *Nat. Cell Biol.*, vol. 18, p. 246, Feb. 2016.
[35] Y. Yin and D. Zhou, "Organoid and Enteroid Modeling of Salmonella Infection," *Front. Cell. Infect. Microbiol.*, vol. 8, Apr. 2018.
[36] K. Ettayebi *et al.*, "Replication of human noroviruses in stem cell–derived human enteroids," *Science*, vol. 353, no. 6306, p. 1387, Sep. 2016.
[37] S. Ranganathan, M. Doucet, C. L. Grassel, B. Delaine-Elias, N. C. Zachos, and E. M. Barry, "Evaluating Shigella flexneri Pathogenesis in the Human Enteroid Model," *Infect. Immun.*, vol. 87, no. 4, pp. e00740-18, Mar. 2019.
[38] B. J. Koestler, C. M. Ward, C. R. Fisher, A. Rajan, A. W. Maresso, and S. M. Payne, "Human Intestinal Enteroids as a Model System of Shigella Pathogenesis," *Infect. Immun.*, vol. 87, no. 4, pp. e00733-18, Apr. 2019.
[39] F. M. Kuhlmann, S. Santhanam, P. Kumar, Q. Luo, M. A. Ciorba, and J. M. Fleckenstein, "Blood Group O–Dependent Cellular Responses to Cholera Toxin: Parallel Clinical and Epidemiological Links to Severe Cholera," *Am. J. Trop. Med. Hyg.*, vol. 95, no. 2, pp. 440–443, Aug. 2016.
[40] R. A. Finkelstein, "Cholera, Vibrio cholerae O1 and O139, and Other Pathogenic Vibrios," in *Medical Microbiology*, 4th ed., S. Baron, Ed. Galveston (TX): University of Texas Medical Branch at Galveston, 1996.
[41] S. A. Jung, C. A. Chapman, and W.-L. Ng, "Quadruple Quorum-Sensing Inputs Control Vibrio cholerae Virulence and Maintain System Robustness," *PLOS Pathog.*, vol. 11, no. 4, p. e1004837, Apr. 2015.
[42] Y. Chen, W. Zhou, T. Roh, M. K. Estes, and D. L. Kaplan, "In vitro enteroid-derived three-dimensional tissue model of human small intestinal epithelium with innate immune responses," *PLOS ONE*, vol. 12, no. 11, p. e0187880, Nov. 2017.
[43] H.-R. Chen and T.-M. Yeh, "In vitro Assays for Measuring Endothelial Permeability by Transwells and Electrical Impedance Systems," *Bio-Protoc.*, vol. 7, no. 9, p. e2273, May 2017.
[44] K. Duval *et al.*, "Modeling Physiological Events in 2D vs. 3D Cell Culture," *Physiol. Bethesda Md*, vol. 32, no. 4, pp. 266–277, Jul. 2017.
[45] J. Zhu, M. B. Miller, R. E. Vance, M. Dziejman, B. L. Bassler, and J. J. Mekalanos, "Quorum-sensing regulators control virulence gene expression in Vibrio cholerae," *Proc. Natl. Acad. Sci.*, vol. 99, no. 5, pp. 3129–3134, Mar. 2002.
[46] B. A. Jude, R. M. Martinez, K. Skorupski, and R. K. Taylor, "Levels of the secreted Vibrio cholerae attachment factor GbpA are modulated by quorum-sensing-induced proteolysis," *J. Bacteriol.*, vol. 191, no. 22, p. 2, Nov. 2009.

[47] M. B. Miller, K. Skorupski, D. H. Lenz, R. K. Taylor, and B. L. Bassler, “Parallel Quorum Sensing Systems Converge to Regulate Virulence in Vibrio cholerae,” *Cell*, vol. 110, no. 3, pp. 303–314, Aug. 2002.
[48] S. Fujii *et al.*, “PGE(2) is a direct and robust mediator of anion/fluid secretion by human intestinal epithelial cells,” *Sci. Rep.*, vol. 6, pp. 36795–36795, Nov. 2016.
[49] F. Rivera-Chávez and J. J. Mekalanos, “Cholera toxin promotes pathogen acquisition of host-derived nutrients,” *Nature*, vol. 572, no. 7768, pp. 244–248, Aug. 2019.
[50] K. Wachsmuth, P. A. Blake, and Ø. Olsvik, Eds., *Vibrio cholerae and cholera: molecular to global perspectives*. Washington, D.C: ASM Press, 1994.
[51] G. Jonson, J. Holmgren, and A.-M. Svennerholm, “Identification of a mannose-binding pilus on Vibrio cholerae El Tor,” *Microb. Pathog.*, vol. 11, no. 6, pp. 433–441, Dec. 1991.